Beyond the Fröhlich Hamiltonian: Path-integral treatment of large polarons in anharmonic solids

Matthew Houtput and Jacques Tempere
Theory of Quantum Systems and Complex Systems, Universiteit Antwerpen, B-2000 Antwerpen, Belgium

(Received 1 December 2020; revised 3 March 2021; accepted 29 April 2021; published 11 May 2021)

The properties of an electron in a typical solid are modified by the interaction with the crystal ions, leading to the formation of a quasiparticle: the polaron. Such polarons are often described using the Fröhlich Hamiltonian, which assumes the underlying lattice phonons to be harmonic. However, this approximation is invalid in several interesting materials, including the recently discovered high-pressure hydrides which superconduct at temperatures above 200 K. In this paper, we show that Fröhlich theory can be extended to eliminate this problem. We derive four additional terms in the Fröhlich Hamiltonian to account for anharmonicity up to third order. We calculate the energy and effective mass of the new polaron, using both perturbation theory and Feynman's path-integral formalism. It is shown that the anharmonic terms lead to significant additional trapping of the electron. The derived Hamiltonian is well suited for analytical calculations, due to its simplicity and since the number of model parameters is low. Since it is a direct extension of the Fröhlich Hamiltonian, it can readily be used to investigate the effect of anharmonicity on other polaron properties, such as the optical conductivity and the formation of bipolarons.

DOI: 10.1103/PhysRevB.103.184306

I. INTRODUCTION

The polaron concept was introduced by Landau [1] and Pekar [2] to explain the dynamics of an electron interacting with a crystal lattice. Classically, the electron-phonon interaction can be explained by the electron displacing the ions out of their equilibrium positions, creating a polarization field that interacts with the electron. The entire system can be described as a quasiparticle: the polaron [1]. It is one of the simplest models describing an impurity interacting with a boson bath, and thus finds applications in many other fields of physics. Specific examples include spin polarons [3], magnetic polarons [4], exciton polarons [5], and the Bose [6–8] and Fermi [9] polaron in ultracold gases.

Usually, the harmonic approximation is made when discussing polarons. One can assume that the lattice potential around an ion's equilibrium position is approximately quadratic, so the restoring forces are linear. This results in a bath of phonons that do not directly interact with each other. This approximation is justified in most materials as the phonon amplitude is usually small. If the electron wave function extends over many unit cells, the lattice can be viewed as a continuous field, and the polaron is called "large." The Hamiltonian for large polarons in the harmonic approximation is known as the Fröhlich Hamiltonian; it is one of the simplest nontrivial Hamiltonians of quantum field theory. Treating the electron in first quantization and the phonons in second quantization, it reads [10]

$$\begin{aligned}\hat{H} &= \hat{H}_{\mathrm{e}} + \hat{H}_{\mathrm{ph}} + \hat{H}_{\mathrm{e-ph}} \\ &= \frac{\hat{\mathbf{p}}_{\mathrm{el}}^2}{2m} + \sum_{\mathbf{k}} \hbar\omega_{\mathbf{k}} \left(\hat{b}_{\mathbf{k}}^\dagger \hat{b}_{\mathbf{k}} + \frac{1}{2} \right) \\ &\quad + \sum_{\mathbf{k}} (V_{\mathbf{k}} \hat{b}_{\mathbf{k}}^\dagger e^{-i\mathbf{k}\cdot\hat{\mathbf{r}}_{\mathrm{el}}} + V_{\mathbf{k}}^* \hat{b}_{\mathbf{k}} e^{i\mathbf{k}\cdot\hat{\mathbf{r}}_{\mathrm{el}}}). \end{aligned} \tag{1}$$

Here, $\omega_{\mathbf{k}}$ is the phonon dispersion and $V_{\mathbf{k}}$ is the electron-phonon interaction strength: Both are functions of the phonon momentum $\mathbf{k}$. The specific form of these functions depends on the system at hand and can significantly alter the underlying physics of the problem [11,12]. The operators $\hat{b}_{\mathbf{k}}^\dagger$ and $\hat{b}_{\mathbf{k}}$ create and annihilate a phonon with wave number $\mathbf{k}$, respectively. A defining characteristic of the Fröhlich Hamiltonian is that $\hat{H}_{\mathrm{ph}}$ is quadratic and $\hat{H}_{\mathrm{e-ph}}$ is linear in the phonon operators.

In reality, the lattice potential is not harmonic, which must be considered when looking at high-pressure hydrides [13–15]. In the classical picture, since the mass of hydrogen ions is small, the phonon amplitude will be too large for the harmonic approximation to apply. Interest in high-pressure hydrides has been strongly renewed since the discovery of high-temperature superconductivity in sulfur hydride [16] ($T_c = 203$ K), lanthanum hydride [17] ($T_c = 260$ K), and carbonaceous sulfur hydride [18] ($T_c = 288$ K) when these materials are put under megabar pressures. Similarly, pure hydrogen has been theoretically predicted to metallize and superconduct at room temperature under the high pressure [19–21]. Superconductivity in these materials appears to be conventional and thus phonon mediated [16]. However, the harmonic approximation is not applicable [13–15], so additional "anharmonic" terms must be considered in the electron-phonon Hamiltonian (1).

Most of the research on anharmonic polarons focuses on "small" polarons [22–24], where the electron is localized around a single lattice atom. The most recent, and to our knowledge only, investigation of the anharmonic terms for large polarons is due to Kussow [25]. In [25], the dominant anharmonic term for the Fröhlich Hamiltonian (1) is derived, and the polaron energy is calculated using perturbation theory in the weak coupling regime. However, the Hamiltonian is only useful for qualitative calculations due to several

assumptions and errors in its derivation. In this paper, we redo the derivation presented in [25], fixing these errors and including the three-phonon terms. Additionally, we will calculate the polaron energy using Feynman's path-integral method [26], allowing us to look at the intermediate coupling and strong coupling regimes as well. The presented Hamiltonian can be used to calculate polaron properties in high-pressure hydrides [16–18], but also in anharmonic semiconductors such as boron nitride [27] and aluminium nitride [28,29].

The structure of this paper is as follows. We derive additional anharmonic terms in the Fröhlich Hamiltonian (1) in Sec. II. In Secs. III and IV, the ground-state energy and effective mass of a single large anharmonic polaron are calculated, using perturbation theory in Sec. III and Feynman's path-integral method [26] in Sec. IV. We summarize our findings in Sec. V.

II. THE ANHARMONIC POLARON HAMILTONIAN

A. Derivation

Here, we rederive the Hamiltonian based on the derivations of Fröhlich [10] and Kussow [25]. We assume the same model system used in both of these derivations: an ionic, polarizable lattice with two ions in the primitive unit cell. The masses of the two ions are denoted with m_1 and m_2. One or more electrons with band mass m and charge $-e$ are placed in this lattice at positions $\mathbf{r}_{\mathrm{el},i}$. We assume that electron-phonon coupling is dominated by the longitudinal optical (LO) phonons, so all other phonon contributions are neglected. The displacements of the ions from their equilibrium positions are denoted by $\mathbf{r}_1$ and $\mathbf{r}_2$, where the position of each ion is measured relative to its respective equilibrium position. The kinetic energy per unit volume due to these displacements is given by

$$E_k = \frac{1}{V_0}\left(\frac{1}{2}m_1\dot{\mathbf{r}}_1^2 + \frac{1}{2}m_2\dot{\mathbf{r}}_2^2\right), \tag{2}$$

where V_0 is the volume of the unit cell. We now switch to center-of-mass coordinates. The movement of the center of mass leads to acoustic phonons and can therefore be neglected [25]. The kinetic energy density can then be written in terms of only the relative displacement $\mathbf{w}$,

$$E_k = \frac{1}{2}\dot{\mathbf{w}}^2, \tag{3}$$

$$\mathbf{w} := \sqrt{\frac{1}{V_0}\frac{m_1 m_2}{m_1+m_2}}(\mathbf{r_2}-\mathbf{r_1}). \tag{4}$$

Since we consider large polarons, the lattice can be approximated by a polarizable continuum. Mathematically, this means we can treat $\mathbf{w} = \mathbf{w}(\mathbf{r})$ as a position-dependent vector field.

Aside from the kinetic energy, the lattice also has an interaction energy U per unit volume. This internal energy contains the interaction energy of the ions, but also a contribution due to the electric displacement field $\mathbf{D}$, which is solely due to the electrons. The internal energy is a function of $\mathbf{w}$ and $\mathbf{D}$ [30], and satisfies

$$dU = -\ddot{\mathbf{w}}\cdot d\mathbf{w} + \mathbf{E}\cdot d\mathbf{D}. \tag{5}$$

Here, $\ddot{\mathbf{w}}$ is proportional to the force on the atoms and $\mathbf{E}$ is the electric field. Both $\mathbf{D} = \mathbf{D}(\mathbf{r},t)$ and $\mathbf{E} = \mathbf{E}(\mathbf{r},t)$ are position and time dependent, just like the relative displacement $\mathbf{w}(\mathbf{r},t)$; however, from now on, we will drop this explicit dependence and simply write $\mathbf{D}$, $\mathbf{E}$, and $\mathbf{w}$.

Since $\mathbf{w} = \mathbf{D} = \mathbf{0}$ corresponds to the equilibrium position of the lattice, the function $\tilde{U}$ can be expanded in powers of $\mathbf{w}$ and $\mathbf{D}$. The first nontrivial order is an expansion up to second order, which is the harmonic expansion that will yield the Fröhlich Hamiltonian (1). In this paper, we consider the internal energy up to third order. It can be written as

$$\begin{aligned} U(\mathbf{w},\mathbf{D}) \approx{}& \tfrac{1}{2}\gamma_{ij}^{(0)}w_i w_j + \gamma_{ij}^{(1)}w_i D_j + \tfrac{1}{2}\gamma_{ij}^{(2)}D_i D_j \\ &+ \tfrac{1}{6}A_{ijl}^{(0)}w_i w_j w_l + \tfrac{1}{2}A_{ijl}^{(1)}w_i w_j D_l + \tfrac{1}{2}A_{ijl}^{(2)}w_i D_j D_l \\ &+ \tfrac{1}{6}A_{ijl}^{(3)}D_i D_j D_l, \end{aligned} \tag{6}$$

where the indices i, j, l can take the values in $\{x, y, z\}$. We use the Einstein summation convention of implied summation over repeated indices throughout the remainder of this article. Contrary to Kussow [25], we expand the internal energy as a function of $\mathbf{D}$ instead of $\mathbf{E}$. The two methods are equivalent since the expansion coefficients are related to each other. The final term is proportional to $\mathbf{D}^3$ and is responsible for the nonlinear optical response of the material. It can be neglected in most materials, but it will be carried here for completeness.

In this expression, second-order tensors $\gamma_{ij}^{(n)}$ and third-order tensors $A_{ijk}^{(n)}$ appear. These tensors can be interpreted as material parameters: in fact, in Sec. II C, we will show that $\gamma_{ij}^{(0)}$, $\gamma_{ij}^{(1)}$, and $\gamma_{ij}^{(2)}$ can be written in terms of measurable quantities for a cubic crystal. In general, these parameters can be calculated using *ab initio* methods by calculating the mixed partial derivatives of the internal energy with respect to $\mathbf{w}$ and $\mathbf{D}$. The tensors $\gamma_{ij}^{(0)}$, $\gamma_{ij}^{(2)}$, $A_{ijk}^{(0)}$, and $A_{ijk}^{(3)}$ are totally symmetric, and the tensors $A_{ijk}^{(1)}$ and $A_{ijk}^{(2)}$ are symmetric in one pair of their indices:

$$A_{ijk}^{(1)} = A_{jik}^{(1)}, \tag{7}$$

$$A_{ijk}^{(2)} = A_{ikj}^{(2)}. \tag{8}$$

In the most general case, the tensor $\gamma_{ij}^{(1)}$ has no symmetry.

We now introduce N free electrons in the system. We assume a parabolic energy dispersion with band mass m. Their kinetic energy takes the standard form,

$$E_{\mathrm{el}} = \sum_{i=1}^{N}\frac{\mathbf{p}_{\mathrm{el},i}^2}{2m}. \tag{9}$$

We note that this form is only valid for cubic crystals, but the band mass m can readily be replaced with an effective inverse mass tensor to account for anisotropy. Integrating the energy densities (3) and (6) over the crystal volume V and adding the electron kinetic energy (9), we obtain the classical Hamiltonian of the system,

$$H = \sum_{i=1}^{N}\frac{\mathbf{p}_{\mathrm{el},i}^2}{2m} + \int_V \frac{1}{2}\dot{\mathbf{w}}\cdot\dot{\mathbf{w}}d^3\mathbf{r} + \int_V U(\mathbf{w},\mathbf{D})d^3\mathbf{r}. \tag{10}$$

All that remains is to find expressions for the phonon field $\mathbf{w}$ and the electric displacement field $\mathbf{D}$.

The longitudinal component of the electric displacement field is only due to the electrons. Its transverse component is zero [10], since **E** and the polarization field **P** are both longitudinal: This follows from the quasistatic third Maxwell equation and the fact that we consider longitudinal phonons, respectively. Therefore, the electric displacement field has an analytical expression [10],

$$\mathbf{D}(\mathbf{r}) = \sum_{i=1}^{N} \frac{e}{4\pi} \nabla \left(\frac{1}{|\mathbf{r} - \mathbf{r}_{\mathrm{el},i}|} \right). \tag{11}$$

For future calculations, it will be useful to write the displacement field in Fourier space as follows:

$$\mathbf{D}(\mathbf{r}) = -\frac{ie}{V} \sum_{\mathbf{k}\neq\mathbf{0}} \frac{\mathbf{n}^{\mathbf{k}}}{|\mathbf{k}|} \rho_{\mathbf{k}} e^{-i\mathbf{k}\cdot\mathbf{r}}, \tag{12}$$

where

$$\rho_{\mathbf{k}} = \sum_{i=1}^{N} e^{i\mathbf{k}\cdot\mathbf{r}_{\mathrm{el},i}} \tag{13}$$

is the density operator of the electrons, and we also introduced the symbol $\mathbf{n}^{\mathbf{k}} = \frac{\mathbf{k}}{|\mathbf{k}|}$ for the unit vector in the direction of $\mathbf{k}$. We will write their components as

$$n_i^{\mathbf{k}} = \frac{k_i}{|\mathbf{k}|}. \tag{14}$$

These unit vectors will feature often in our calculations and results.

Up to a proportionality constant, the field $\mathbf{w}$ can be interpreted as a phonon coordinate. Its conjugate momentum is simply $\frac{\partial H}{\partial \dot{\mathbf{w}}} = \dot{\mathbf{w}}$. We can quantize $\mathbf{w}$ and $\dot{\mathbf{w}}$ using the ladder operators $\hat{b}_{\mathbf{k}}$ and $\hat{b}_{\mathbf{k}}^{\dagger}$, if we can identify the phonon frequencies. Rather than derive an equation for the polarization density **P** as is done in [10,25], we do this by looking at the Hamiltonian (10) in the case of no electrons: $\mathbf{D} = \mathbf{0}$. Furthermore, we only look at the harmonic approximation, so we only use the first line of Eq. (6). The Hamiltonian density then takes the form of a harmonic oscillator,

$$\mathcal{H} = \tfrac{1}{2}\dot{\mathbf{w}} \cdot \dot{\mathbf{w}} + \tfrac{1}{2}\mathbf{w} \cdot \boldsymbol{\gamma}_0 \cdot \mathbf{w}, \tag{15}$$

where the bold $\boldsymbol{\gamma}_0$ indicates the matrix with components $\gamma_{ij}^{(0)}$. Since the matrix $\boldsymbol{\gamma}_0$ is symmetric, it can be diagonalized. Its eigenvectors are the eigendirections of the phonons, and its eigenvalues ω_i^2 are the squares of the phonon frequencies. Therefore, if we write $\boldsymbol{\gamma}_0 = \boldsymbol{\Omega}^2$, the matrix $\boldsymbol{\Omega}$ can be used instead of the phonon frequency in the definition of the ladder operators.

To find an expression for $\mathbf{w}$ and $\dot{\mathbf{w}}$ in terms of the ladder operators, we introduce an auxiliary field $\mathbf{B}(\mathbf{r})$ and its Fourier transform $\hat{b}_{\mathbf{k}}$ after Fröhlich [10],

$$\mathbf{B}(\mathbf{r}) = \frac{1}{i}\sqrt{\frac{1}{2\hbar}}\boldsymbol{\Omega}^{\frac{1}{2}}[\mathbf{w}(\mathbf{r}) + i\boldsymbol{\Omega}^{-1}\dot{\mathbf{w}}(\mathbf{r})], \tag{16}$$

$$\mathbf{B}(\mathbf{r}) = \frac{1}{\sqrt{V}} \sum_{\mathbf{k}\neq\mathbf{0}} \mathbf{n}^{\mathbf{k}} \hat{b}_{\mathbf{k}} e^{i\mathbf{k}\cdot\mathbf{r}}. \tag{17}$$

The equations for $\mathbf{B}(\mathbf{r})$ and $\mathbf{B}^*(\mathbf{r})$ can be inverted to obtain the following explicit expressions for $\mathbf{w}$ and $\dot{\mathbf{w}}$:

$$\mathbf{w}(\mathbf{r}) = -i\sqrt{\frac{\hbar}{2V}}\boldsymbol{\Omega}^{-\frac{1}{2}} \sum_{\mathbf{k}\neq\mathbf{0}} \mathbf{n}^{\mathbf{k}} (\hat{b}_{\mathbf{k}}^{\dagger} + \hat{b}_{-\mathbf{k}}) e^{-i\mathbf{k}\cdot\mathbf{r}}, \tag{18}$$

$$\dot{\mathbf{w}}(\mathbf{r}) = \sqrt{\frac{\hbar}{2V}}\boldsymbol{\Omega}^{\frac{1}{2}} \sum_{\mathbf{k}\neq\mathbf{0}} \mathbf{n}^{\mathbf{k}} (\hat{b}_{\mathbf{k}}^{\dagger} - \hat{b}_{-\mathbf{k}}) e^{-i\mathbf{k}\cdot\mathbf{r}}. \tag{19}$$

These expressions will be used to eliminate $\mathbf{w}$ in the Hamiltonian (10). Classically, $\hat{b}_{\mathbf{k}}$ and $\hat{b}_{\mathbf{k}}^{\dagger}$ are the Fourier transforms of the unknown auxiliary fields $\mathbf{B}(\mathbf{r})$ and $\mathbf{B}^*(\mathbf{r})$. In order to quantize the phonon field, we have to impose the canonical commutation relations,

$$[w_j(\mathbf{r}), \dot{w}_k(\mathbf{r}')] = i\hbar\delta_{jk}\delta(\mathbf{r} - \mathbf{r}'). \tag{20}$$

It can be shown [10] that these canonical commutation relations hold if $\hat{b}_{\mathbf{k}}$ and $\hat{b}_{\mathbf{k}}^{\dagger}$ satisfy the bosonic commutation relations. Therefore, we can interpret $\hat{b}_{\mathbf{k}}^{\dagger}$ and $\hat{b}_{\mathbf{k}}$ as the creation and annihilation operator of the phonon field, respectively. To complete the quantization, we have to turn $\mathbf{r}_{\mathrm{el},i}$ and $\mathbf{p}_{\mathrm{el},i}$ into operators, which obey the usual commutation relations. We now combine Eq. (6) for the interaction energy density, (10) for the classical Hamiltonian, (12) for the electric displacement field, and (18) and (19) for $\mathbf{w}$ and $\dot{\mathbf{w}}$ in order to find the quantum mechanical Hamiltonian. The volume integrals are all of the form

$$\int_V e^{i\mathbf{K}\cdot\mathbf{r}} d^3\mathbf{r} = V\delta_{\mathbf{K},0}. \tag{21}$$

Then, a straightforward calculation gives the following Hamiltonian:

$$\begin{aligned}
\hat{H} = &\sum_{i=1}^{N} \frac{\hat{\mathbf{p}}_{\mathrm{el},i}^2}{2m} + \sum_{\mathbf{k}} \hbar\omega_{\mathbf{k}} \left(\hat{b}_{\mathbf{k}}^{\dagger}\hat{b}_{\mathbf{k}} + \frac{1}{2} \right) \\
&+ \frac{1}{2} \sum_{\mathbf{k}\neq\mathbf{0}} V_{\mathbf{k}}^{(C)} \hat{\rho}_{\mathbf{k}}\hat{\rho}_{-\mathbf{k}} + \sum_{\mathbf{k}\neq\mathbf{0}} V_{\mathbf{k}}^{(F)} (\hat{b}_{\mathbf{k}}^{\dagger} + \hat{b}_{-\mathbf{k}})\hat{\rho}_{-\mathbf{k}} \\
&+ \sum_{\mathbf{k}\neq\mathbf{q}\neq\mathbf{0}} V_{\mathbf{k},\mathbf{q}}^{(0)} (\hat{b}_{-\mathbf{k}}^{\dagger} + \hat{b}_{\mathbf{k}})(\hat{b}_{\mathbf{k}-\mathbf{q}}^{\dagger} + \hat{b}_{-\mathbf{k}+\mathbf{q}})(\hat{b}_{\mathbf{q}}^{\dagger} + \hat{b}_{-\mathbf{q}}) \\
&+ \sum_{\mathbf{k}\neq\mathbf{q}\neq\mathbf{0}} V_{\mathbf{k},\mathbf{q}}^{(1)} (\hat{b}_{-\mathbf{k}}^{\dagger} + \hat{b}_{\mathbf{k}})(\hat{b}_{\mathbf{q}}^{\dagger} + \hat{b}_{-\mathbf{q}})\hat{\rho}_{\mathbf{k}-\mathbf{q}} \\
&+ \sum_{\mathbf{k}\neq\mathbf{q}\neq\mathbf{0}} V_{\mathbf{k},\mathbf{q}}^{(2)} (\hat{b}_{\mathbf{k}-\mathbf{q}}^{\dagger} + \hat{b}_{-\mathbf{k}+\mathbf{q}})\hat{\rho}_{-\mathbf{k}}\hat{\rho}_{\mathbf{q}} \\
&+ \sum_{\mathbf{k}\neq\mathbf{q}\neq\mathbf{0}} V_{\mathbf{k},\mathbf{q}}^{(3)} \hat{\rho}_{-\mathbf{k}}\hat{\rho}_{\mathbf{k}-\mathbf{q}}\hat{\rho}_{\mathbf{q}},
\end{aligned} \tag{22}$$

where the sums exclude the cases where $\mathbf{k} = \mathbf{0}$, $\mathbf{q} = \mathbf{0}$, and $\mathbf{k} = \mathbf{q}$; this can also be taken into account by requiring that $V_{\mathbf{0}}^{(F)} = 0$, $V_{\mathbf{k},\mathbf{k}}^{(n)} = 0$, and so on. The phonon frequency $\omega_{\mathbf{k}}$ is given by

$$\omega_{\mathbf{k}} = \mathbf{n}^{\mathbf{k}} \cdot \boldsymbol{\Omega} \cdot \mathbf{n}^{\mathbf{k}}. \tag{23}$$

Furthermore, we define $\mathbf{\Lambda} := \mathbf{\Omega}^{-\frac{1}{2}} = \boldsymbol{\gamma}_0^{-\frac{1}{4}}$ and the following interaction strengths, which have the dimensions of energy and are analytical functions of $\mathbf{k}$ and $\mathbf{q}$:

$$V_{\mathbf{k}}^{(C)} = \frac{e^2}{V}\frac{\mathbf{n}^{\mathbf{k}}\cdot\boldsymbol{\gamma}_2\cdot\mathbf{n}^{\mathbf{k}}}{|\mathbf{k}|^2}, \tag{24}$$

$$V_{\mathbf{k}}^{(F)} = \sqrt{\frac{\hbar e^2}{2V}}\frac{\mathbf{n}^{\mathbf{k}}\cdot(\mathbf{\Lambda}\cdot\boldsymbol{\gamma}_1)\cdot\mathbf{n}^{\mathbf{k}}}{|\mathbf{k}|}, \tag{25}$$

$$V_{\mathbf{k},\mathbf{q}}^{(0)} = \frac{-i}{6\sqrt{V}}\left(\frac{\hbar}{2}\right)^{\frac{3}{2}}\left[\Lambda_{ia}\Lambda_{jb}\Lambda_{lc}A_{abc}^{(0)}\right]n_i^{\mathbf{k}}n_j^{\mathbf{k}-\mathbf{q}}n_l^{\mathbf{q}}, \tag{26}$$

$$V_{\mathbf{k},\mathbf{q}}^{(1)} = \frac{-ie\hbar}{4V}\left[\Lambda_{ia}\Lambda_{jb}A_{abl}^{(1)}\right]\frac{n_i^{\mathbf{k}}n_j^{\mathbf{q}}n_l^{\mathbf{k}-\mathbf{q}}}{|\mathbf{k}-\mathbf{q}|}, \tag{27}$$

$$V_{\mathbf{k},\mathbf{q}}^{(2)} = \frac{-ie^2}{2V^{\frac{3}{2}}}\sqrt{\frac{\hbar}{2}}\left[\Lambda_{ia}A_{ajl}^{(2)}\right]\frac{n_i^{\mathbf{k}-\mathbf{q}}n_j^{\mathbf{k}}n_l^{\mathbf{q}}}{|\mathbf{k}||\mathbf{q}|}, \tag{28}$$

$$V_{\mathbf{k},\mathbf{q}}^{(3)} = \frac{-ie^3}{6V^2}A_{ijl}^{(3)}\frac{n_i^{\mathbf{k}}n_j^{\mathbf{k}-\mathbf{q}}n_l^{\mathbf{q}}}{|\mathbf{k}||\mathbf{k}-\mathbf{q}||\mathbf{q}|}. \tag{29}$$

The Hamiltonian given by (22) is a general Hamiltonian for N large polarons interacting with a boson bath, including interaction terms up to third order. The first line is the Fröhlich Hamiltonian (1), extended to include multiple electrons. We note that the kinetic energy of the electrons can be replaced by a more general energy band, for example one with an anisotropic band mass. The other lines are the third-order anharmonic correction terms to the Hamiltonian. All of the terms can be visualized using Feynman diagrams, which is done in Fig. 1.

For coupling to a single LO phonon mode in a crystal with arbitrary symmetry, the interaction strengths appearing in this Hamiltonian are given by Eqs. (24)–(29). In order, these correspond to the Coulomb interaction (24), the Fröhlich interaction (25), and the anharmonic processes involving anywhere from 0 to 3 electrons and phonons (26)–(29). As expected, the Coulomb interaction strength goes as $\frac{1}{|\mathbf{k}|^2}$ and the Fröhlich interaction goes as $\frac{1}{|\mathbf{k}|}$; however, the proportionality constant can have an angular dependence if the crystal is not cubic. The functions $V_{\mathbf{k},\mathbf{q}}^{(n)}$ are more complicated, but still analytical. Expression (27) for the interaction strength $V_{\mathbf{k},\mathbf{q}}^{(1)}$ does not agree with the result found by Kussow [25]: We will discuss this difference in Sec. V.

The anharmonic interaction strengths $V_{\mathbf{k},\mathbf{q}}^{(n)}$ are all purely imaginary. This can be understood by requiring that the Hamiltonian (22) be Hermitian, which leads to the conditions

$$V_{\mathbf{k}}^{(F)*} = V_{-\mathbf{k}}^{(F)}, \tag{30}$$

$$V_{\mathbf{k},\mathbf{q}}^{(n)*} = V_{-\mathbf{k},-\mathbf{q}}^{(n)}. \tag{31}$$

Since the third-order terms are antisymmetric in $\mathbf{k}$ and $\mathbf{q}$, the imaginary unit is required for a Hermitian Hamiltonian.

The energy density was expanded up to third order, which means the Hamiltonian (22) is, in principle, unstable if the phonon displacements become too large. As long as the phonons are approximately harmonic and the third-order terms can be seen as correction terms, we do not expect this situation to occur. Regardless, a stable Hamiltonian can be obtained by expanding the interaction energy density (6) up to fourth or even higher order. Expressions (10), (12), and (18) can then be used to obtain a Hamiltonian up to arbitrary order.

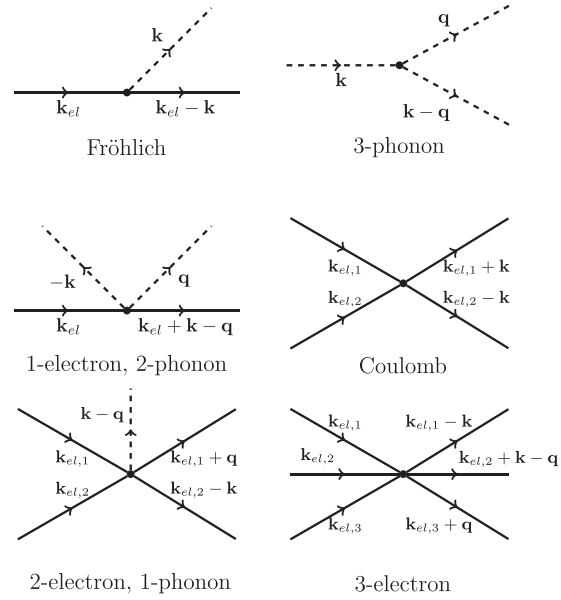

FIG. 1. A representation of the different interaction terms (22) using Feynman diagrams. Solid lines represent electrons and dashed lines represent phonons. In these diagrams, any phonon line may have its arrow and momentum reversed to create a new diagram: e.g., for the Fröhlich interaction, the electron can also absorb a phonon with momentum $-\mathbf{k}$. For a single polaron, only the first three interactions must be considered. The three-electron interaction is linked to the nonlinear optical response and can therefore be neglected in most materials.

B. Symmetry constraints

Equation (6) was proposed for an arbitrary crystal. However, the symmetry of the crystal enforces additional constraints onto the tensors $\gamma_{ij}^{(n)}$ and $A_{ijl}^{(n)}$ in this expression. Here, we aim to find the simplest possible form of these tensors for a crystal with cubic symmetry.

Consider a unit cell, centered at $\mathbf{r}$, with a relative displacement $\mathbf{w}$ and electric displacement field $\mathbf{D}$. In the continuum limit, $\mathbf{w}$ and $\mathbf{D}$ can be considered constant over the entire unit cell. If a crystal symmetry transformation R is applied to both $\mathbf{w}$ and $\mathbf{D}$, the resulting unit cell is the same as if we had simply applied R to the entire system. Therefore, it must hold that

$$U(R\cdot\mathbf{w}, R\cdot\mathbf{D}) = U(\mathbf{w},\mathbf{D}), \tag{32}$$

for all crystal symmetries R. Note that only the rotational part of R is relevant: Translations can be neglected since $\mathbf{w}$ and $\mathbf{D}$ vary little over the size of one unit cell. Therefore, R can be represented by a 3×3 matrix, and only the point group $\mathscr{G}$ of the crystal must be considered.

Combining Eqs. (6) and (32), the following constraints on the tensors $\gamma_{ij}^{(n)}$ and $A_{ijl}^{(n)}$ are obtained:

$$\forall R\in\mathscr{G}: \gamma_{ij}^{(n)} = R_{ia}R_{jb}\gamma_{ab}^{(n)}, \tag{33}$$

$$A_{ijk}^{(n)} = R_{ia}R_{jb}R_{kc}A_{abc}^{(n)}. \tag{34}$$

In other words, the tensors must be invariant under all lattice symmetry transformations. It can be immediately verified that if $\gamma_{ij}^{(n)}$ or $A_{ijl}^{(n)}$ is invariant under two different lattice transformations R_1 and R_2, it is also invariant under $R_1 \cdot R_2$.

We apply these equations to two important cases: the case where the crystal has inversion symmetry and the case of cubic point groups. The inversion operator can be represented with the matrix $R_{ij} = -\delta_{ij}$. Therefore, if the crystal has inversion symmetry, Eq. (34) immediately gives $A_{ijk}^{(n)} = 0$. In this case, all of the third-order anharmonic terms in the Hamiltonian (22) are identically zero, and the Hamiltonian reduces to the Fröhlich Hamiltonian. The scope of this article is therefore limited to crystals without inversion symmetry; to investigate anharmonicity in symmetric crystals, the internal energy density (6) must be expanded to fourth order.

To investigate the case of cubic symmetry, we start with the smallest cubic point group: the symmetry group of a tetrahedron (denoted in Hermann-Mauguin notation as 23). It is generated by two elements:

$$R_1 = \begin{pmatrix} -1 & 0 & 0 \\ 0 & -1 & 0 \\ 0 & 0 & 1 \end{pmatrix}, \quad R_2 = \begin{pmatrix} 0 & 0 & 1 \\ 1 & 0 & 0 \\ 0 & 1 & 0 \end{pmatrix}. \tag{35}$$

Since the entire group can be generated by products of these elements, it suffices to find tensors $\gamma_{ij}^{(n)}$ and $A_{ijl}^{(n)}$ that are invariant under these two elements. For a second-order tensor γ_{ij}, only the unit tensor is invariant under both R_1 and R_2,

$$\gamma_{ij}^{(n)} = \gamma_n \delta_{ij}, \tag{36}$$

and so we obtain the familiar result for cubic crystals. For a third-order tensor, the calculation can be simplified by noting that all our third-order tensors must be fully symmetric, since this is implied by invariance under R_2 and either one of the conditions (7) or (8). Again, only one tensor satisfies all of the implied constraints, and that is the absolute value of the Levi-Civita tensor (denoted throughout this article with $\mathcal{E}$),

$$A_{ijl}^{(n)} = A_n \mathcal{E}_{ijl}, \tag{37}$$

$$\mathcal{E}_{ijl} = \begin{cases} 1 & \text{if } i \neq j \neq l, \\ 0 & \text{otherwise.} \end{cases} \tag{38}$$

This tensor is different from the one used in [25]: We postpone the comparison with [25] until Sec. V. The other four cubic symmetry groups ($m\bar{3}$, 432, $\bar{4}3m$, and $m\bar{3}m$) can all be obtained from the group 23 by adding one or more generators. Therefore, for all cubic crystals, the tensors $\gamma_{ij}^{(n)}$ and $A_{ijl}^{(n)}$ are of the form (36) and (37). All of these tensors can be described with a single scalar parameter, which is of great practical importance. This scalar parameter can be identically equal to zero if the symmetry is too high: If the crystal symmetry group is $m\bar{3}$, 432, or $m\bar{3}m$, it holds that $A_n = 0$. Therefore, for the remainder of this article, we will limit ourselves to crystals whose point group is either 23 or $\bar{4}3m$, in addition to the assumptions made during the derivation in Sec. II A. The zinc-blende structure is an important example of a crystal structure that satisfies all of these assumptions.

C. Link to measurable material parameters

In a cubic crystal, the parameters γ_0, γ_1, and γ_2 can be expressed in terms of three familiar material properties: the longitudinal optical phonon frequency ω_0, the relative dielectric constant ε, and the square of the refractive index ε_∞. To find this correspondence, we start from the total energy density up to second order, assuming Eq. (33) for a cubic crystal,

$$\mathcal{H} = \tfrac{1}{2}\dot{\mathbf{w}} \cdot \dot{\mathbf{w}} + \tfrac{1}{2}\gamma_0 \mathbf{w} \cdot \mathbf{w} + \gamma_1 \mathbf{w} \cdot \mathbf{D} + \tfrac{1}{2}\gamma_2 \mathbf{D} \cdot \mathbf{D}. \tag{39}$$

If no electrons are present, $\mathbf{D} = \mathbf{0}$ and we immediately obtain

$$\gamma_0 = \omega_0^2, \tag{40}$$

as before. To find γ_1 and γ_2, we derive the dielectric function for this system. The electric field can be derived from Eq. (5), as well as an equation of motion for $\mathbf{w}$,

$$\mathbf{E} = \frac{\partial H}{\partial \mathbf{D}} = \gamma_1 \mathbf{w} + \gamma_2 \mathbf{D}, \tag{41}$$

$$\ddot{\mathbf{w}} = -\frac{\partial H}{\partial \mathbf{w}} = -\omega_0^2 \mathbf{w} - \gamma_1 \mathbf{D}. \tag{42}$$

We are now interested in the temporal Fourier transforms $\tilde{\mathbf{D}}(\omega)$ and $\tilde{\mathbf{E}}(\omega)$. In Fourier space, the equations of motion become

$$\tilde{\mathbf{E}}(\omega) = \gamma_1 \tilde{\mathbf{w}}(\omega) + \gamma_2 \tilde{\mathbf{D}}(\omega), \tag{43}$$

$$-\omega^2 \tilde{\mathbf{w}}(\omega) = -\omega_0^2 \tilde{\mathbf{w}}(\omega) - \gamma_1 \tilde{\mathbf{D}}(\omega). \tag{44}$$

Here, $\tilde{\mathbf{w}}(\omega)$ can be eliminated from this equation, yielding a linear relation between $\mathbf{D}$ and $\mathbf{E}$. The proportionality constant is the dielectric function, which can be written as

$$\varepsilon(\omega) = \frac{1}{\varepsilon_0 \gamma_2} \left(\frac{\omega^2 - \omega_0^2}{\omega^2 - \omega_0^2 + \frac{\gamma_1^2}{\gamma_2}} \right), \tag{45}$$

where ε_0 is the vacuum permittivity. This dielectric function is of the polariton type, where ω_0 indeed plays the role of the longitudinal optical phonon frequency. From the limits $\varepsilon = \varepsilon(0)$ and $\varepsilon_\infty = \varepsilon(+\infty)$, we obtain

$$\gamma_1 = \omega_0 \sqrt{\frac{1}{\varepsilon_0} \left(\frac{1}{\varepsilon_\infty} - \frac{1}{\varepsilon} \right)}, \tag{46}$$

$$\gamma_2 = \frac{1}{\varepsilon_0 \varepsilon_\infty}. \tag{47}$$

Equations (40), (46), and (47) allow us to eliminate the parameters γ_0, γ_1, and γ_2 for cubic crystals, in favor of the experimentally available parameters ω_0, ε, and ε_∞.

This procedure also allows us to write the phonon frequency (23) and interaction strengths (24)–(29) in a simpler form, where the strength of each interaction is characterized by a single scalar parameter. For example, the Fröhlich interaction strength can be written as

$$V_{\mathbf{k}}^{(F)} = \hbar\omega_0 \sqrt{\frac{4\pi\alpha}{V}} \left(\frac{\hbar}{2m\omega_0} \right)^{1/4} \frac{1}{|\mathbf{k}|}, \tag{48}$$

where the dimensionless Fröhlich coupling constant α is defined as

$$\alpha := \frac{1}{2\hbar\omega_0}\frac{e^2}{4\pi\varepsilon_0}\sqrt{\frac{2m\omega_0}{\hbar}}\left(\frac{1}{\varepsilon_\infty}-\frac{1}{\varepsilon}\right). \tag{49}$$

Both of these correspond to the well-known formulas for a single Fröhlich polaron [10]. Analogously, four new dimensionless anharmonic coupling constants can be defined. If we assume the third-order tensors are of the form (37), define the dimensionless parameters T_0, T_1, T_2, and T_3 as follows:

$$T_n = \frac{(2\omega_0\sqrt{\varepsilon_0})^n}{\hbar\omega_0}\left(\frac{1}{\varepsilon_\infty}-\frac{1}{\varepsilon}\right)^{-\frac{n}{2}}\left(\frac{\hbar m}{2\omega_0}\right)^{\frac{3}{4}}A_n, \tag{50}$$

and introduce the typical polaron length scale,

$$a_p := \sqrt{\frac{\hbar}{2m\omega_0}}, \tag{51}$$

then the phonon frequency and interaction strengths for a cubic crystal can be written in a convenient analytic form,

$$\omega_{\mathbf{k}} = \omega_0, \tag{52}$$

$$V^{(C)}_{\mathbf{k}} = \frac{e^2}{V\varepsilon_0\varepsilon_\infty}\frac{1}{|\mathbf{k}|^2}, \tag{53}$$

$$V^{(F)}_{\mathbf{k}} = \hbar\omega_0\sqrt{\frac{4\pi\alpha a_p}{V}}\frac{1}{|\mathbf{k}|}, \tag{54}$$

$$V^{(0)}_{\mathbf{k},\mathbf{q}} = -i\frac{\hbar\omega_0}{6}\frac{a_p^{\frac{3}{2}}}{\sqrt{V}}T_0\,\mathcal{E}_{ijl}n_i^{\mathbf{k}}n_j^{\mathbf{k}-\mathbf{q}}n_l^{\mathbf{q}}, \tag{55}$$

$$V^{(1)}_{\mathbf{k},\mathbf{q}} = -i\frac{\hbar\omega_0}{2}\frac{\sqrt{4\pi\alpha}a_p^2}{V}T_1\,\mathcal{E}_{ijl}\frac{n_i^{\mathbf{k}}n_j^{\mathbf{k}-\mathbf{q}}n_l^{\mathbf{q}}}{|\mathbf{k}-\mathbf{q}|}, \tag{56}$$

$$V^{(2)}_{\mathbf{k},\mathbf{q}} = -i\frac{\hbar\omega_0}{2}\frac{4\pi\alpha a_p^{\frac{5}{2}}}{V^{\frac{3}{2}}}T_2\,\mathcal{E}_{ijl}\frac{n_i^{\mathbf{k}}n_j^{\mathbf{k}-\mathbf{q}}n_l^{\mathbf{q}}}{|\mathbf{k}||\mathbf{q}|}, \tag{57}$$

$$V^{(3)}_{\mathbf{k},\mathbf{q}} = -i\frac{\hbar\omega_0}{6}\frac{(4\pi\alpha)^{\frac{3}{2}}a_p^3}{V^2}T_3\,\mathcal{E}_{ijl}\frac{n_i^{\mathbf{k}}n_j^{\mathbf{k}-\mathbf{q}}n_l^{\mathbf{q}}}{|\mathbf{k}||\mathbf{k}-\mathbf{q}||\mathbf{q}|}. \tag{58}$$

All of these interaction strengths consist of a prefactor that fixes the units, a dimensionless scalar representing the relative strength of the interaction, and an analytic function of $\mathbf{k}$ and/or $\mathbf{q}$. Unlike the coupling constant α, the anharmonic constants T_0, T_1, T_2, and T_3 cannot be readily written in terms of measurable quantities; however, they can still be obtained from first-principles calculations.

It must be noted that unlike the Coulomb and Fröhlich interactions, the anharmonic interaction strengths are no longer spherically symmetric. Indeed, they have an angular dependence through the components of the unit vectors $n_i^{\mathbf{k}}$, $n_j^{\mathbf{k}-\mathbf{q}}$, and $n_l^{\mathbf{q}}$. Despite this, the dependence on $\mathbf{k}$ and $\mathbf{q}$ is analytic, making these interaction strengths well suited for further theoretical investigations.

For the remainder of this article, we will consider a single polaron. In this case, the density operator becomes

$$\hat{\rho}_{\mathbf{k}} = e^{i\mathbf{k}\cdot\hat{\mathbf{r}}_{\mathrm{el}}}. \tag{59}$$

The diagrams on the bottom row of Fig. 1 all require more than one electron since the electron cannot interact with its own field. Therefore, the three terms in the Hamiltonian corresponding to these diagrams drop out, and we obtain the following simplified Hamiltonian for a single polaron:

$$\hat{H} := \hat{H}_{\mathrm{free}} + \hat{H}_F + \hat{H}_0 + \hat{H}_1, \tag{60}$$

$$\hat{H}_{\mathrm{free}} := \frac{\hat{\mathbf{p}}_{\mathrm{el}}^2}{2m} + \sum_{\mathbf{k}}\hbar\omega_{\mathbf{k}}\left(\hat{b}_{\mathbf{k}}^\dagger\hat{b}_{\mathbf{k}}+\frac{1}{2}\right), \tag{61}$$

$$\hat{H}_F := \sum_{\mathbf{k}\neq\mathbf{0}}V_{\mathbf{k}}^{(F)}(\hat{b}_{\mathbf{k}}^\dagger+\hat{b}_{-\mathbf{k}})\hat{\rho}_{-\mathbf{k}}, \tag{62}$$

$$\hat{H}_0 := \sum_{\mathbf{k}\neq\mathbf{q}\neq\mathbf{0}}V_{\mathbf{k},\mathbf{q}}^{(0)}(\hat{b}_{-\mathbf{k}}^\dagger+\hat{b}_{\mathbf{k}})(\hat{b}_{\mathbf{k}-\mathbf{q}}^\dagger+\hat{b}_{-\mathbf{k}+\mathbf{q}})(\hat{b}_{\mathbf{q}}^\dagger+\hat{b}_{-\mathbf{q}}), \tag{63}$$

$$\hat{H}_1 := \sum_{\mathbf{k}\neq\mathbf{q}\neq\mathbf{0}}V_{\mathbf{k},\mathbf{q}}^{(1)}(\hat{b}_{-\mathbf{k}}^\dagger+\hat{b}_{\mathbf{k}})(\hat{b}_{\mathbf{q}}^\dagger+\hat{b}_{-\mathbf{q}})\hat{\rho}_{\mathbf{k}-\mathbf{q}}. \tag{64}$$

This Hamiltonian, along with the interaction strengths (54)–(56), are the central result of this article. It is the lowest-order generalization to the Fröhlich Hamiltonian (1), making all assumptions of its derivation except for the harmonic approximation. Omitting this approximation gives, to lowest order, two additional interaction terms. The first term (63) is a three-phonon interaction term due to the anharmonicity of the phonons. The second term (64) is an "extended" interaction term, similar to the Fröhlich interaction but involving two phonons. Since the anharmonicity of the phonons can be included in the phonon frequency through first-principles calculations [13–15], the extended interaction term is the more interesting of the two.

III. PERTURBATION THEORY

In this section, we calculate the polaron energy using perturbation theory, up to first order in α and up to second order in T_0 and T_1. The Hamiltonian (62)–(64) can be written as a sum of four contributions (61)–(64). The first contribution has known eigenstates and energy eigenvalues, while the

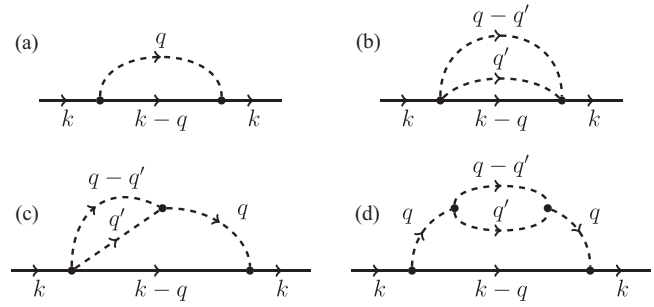

FIG. 2. Diagrammatic representation of the contributions to the polaron self-energy, at zero temperature, and to first order in α and second order in T_0 and T_1. (a) The sunset diagram gives the energy of the Fröhlich polaron. Diagrams (b)–(d) contain two anharmonic interactions. Diagram (c) appears with an extra factor 2 since the order of the interactions can be switched.

other three terms are interaction terms and can be considered "small."

The self-energy contributions are shown in Fig. 2. Full lines represent the electron Green's function G_0, and dashed lines correspond to the phonon Green's function D_0. Two new vertex factors are introduced: $3\sqrt{2}V^{(0)}_{\mathbf{k},\mathbf{q}}$ for the three-phonon vertex, and $\sqrt{2}V^{(1)}_{\mathbf{k},\mathbf{q}}$ for the vertex representing the absorption/emission of two phonons. We obtain, for the self-energies of the different diagrams,

$$\Sigma_a(\mathbf{k},\omega) = \frac{i}{\hbar^2}\int_{-\infty}^{+\infty}\frac{d\nu}{2\pi}\sum_{\mathbf{q}}\left|V^{(F)}_{\mathbf{q}}\right|^2 G_0(\mathbf{k}-\mathbf{q},\omega-\nu)D_0(\nu), \tag{65}$$

$$\Sigma_b(\mathbf{k},\omega) = \frac{2i^2}{\hbar^2}\int_{-\infty}^{+\infty}\frac{d\nu d\nu'}{(2\pi)^2}\sum_{\mathbf{q},\mathbf{q}'}\left|V^{(1)}_{\mathbf{q}'-\mathbf{q},\mathbf{q}'}\right|^2 G_0(\mathbf{k}-\mathbf{q},\omega-\nu)D_0(\nu-\nu')D_0(\nu'), \tag{66}$$

$$\Sigma_c(\mathbf{k},\omega) = \frac{12i^2}{\hbar^3}\int_{-\infty}^{+\infty}\frac{d\nu d\nu'}{(2\pi)^2}\sum_{\mathbf{q},\mathbf{q}'}V^{(F)}_{\mathbf{q}}V^{(0)}_{\mathbf{q},\mathbf{q}'}V^{(1)*}_{\mathbf{q}'-\mathbf{q},\mathbf{q}'}G_0(\mathbf{k}-\mathbf{q},\omega-\nu)D_0(\nu)D_0(\nu-\nu')D_0(\nu'), \tag{67}$$

$$\Sigma_d(\mathbf{k},\omega) = \frac{18i^2}{\hbar^4}\int_{-\infty}^{+\infty}\frac{d\nu d\nu'}{(2\pi)^2}\sum_{\mathbf{q},\mathbf{q}'}\left|V^{(F)}_{\mathbf{q}}\right|^2\left|V^{(0)}_{\mathbf{q},\mathbf{q}'}\right|^2 G_0(\mathbf{k}-\mathbf{q},\omega-\nu)D_0(\nu)^2D_0(\nu-\nu')D_0(\nu'). \tag{68}$$

Adding all the contributions together and using the explicit forms of the interaction strengths (54)–(56), this self-energy can be written rather compactly as follows:

$$\Sigma(\mathbf{k},\omega) = \frac{i}{\hbar^2}\int_{-\infty}^{+\infty}\frac{d\nu}{2\pi}\sum_{\mathbf{q}}\left|V^{(F)}_{\mathbf{q}}\right|^2 G_0(\mathbf{k}-\mathbf{q},\omega-\nu)\left\{D_0(\nu)+\frac{1}{2}\sum_{\mathbf{q}'}\left|\frac{6V^{(0)}_{\mathbf{q},\mathbf{q}'}}{\hbar\omega_0}\right|^2\left[\frac{T_1}{T_0}-\omega_0 D_0(\nu)\right]^2 i\int_{-\infty}^{+\infty}\frac{d\nu'}{2\pi}D_0(\nu-\nu')D_0(\nu')\right\}. \tag{69}$$

In the Appendix, we prove that

$$\sum_{\mathbf{q}'}\left|\frac{6V^{(0)}_{\mathbf{q},\mathbf{q}'}}{\hbar\omega_0}\right|^2 = \frac{4T_0^2}{15\tilde{V}_0}, \tag{70}$$

where the dimensionless volume of the unit cell is defined by

$$\tilde{V}_0 = \frac{V_0}{a_p^3}. \tag{71}$$

The remaining integrals are straightforward and are overall very similar to the self-energy integral for the Fröhlich problem. Introducing the dimensionless variables $\tilde{\mathbf{k}} = a_p\mathbf{k}$ and $\tilde{\omega} = \omega/\omega_0$, the final result for the self-energy becomes

$$\frac{\Sigma(\tilde{\mathbf{k}},\tilde{\omega})}{\omega_0} = -\alpha\left[1+\frac{16T_0}{45\tilde{V}_0}\left(T_1+\frac{T_0}{6}\right)\right]\frac{1}{\tilde{k}}\arctan\left(\frac{\tilde{k}}{\sqrt{1-\tilde{\omega}-i\delta}}\right) \tag{72}$$

$$-\alpha\frac{2}{15\tilde{V}_0}\left(T_1-\frac{2T_0}{3}\right)^2\frac{1}{\tilde{k}}\arctan\left(\frac{\tilde{k}}{\sqrt{2-\tilde{\omega}-i\delta}}\right) \tag{73}$$

$$-\alpha\frac{4T_0^2}{45\tilde{V}_0}\frac{1}{\tilde{k}^2+1-\tilde{\omega}}\frac{1}{\sqrt{1-\tilde{\omega}-i\delta}}+O(\alpha^2). \tag{74}$$

Up to first order in α, the self-energy correction to the dispersion, $E = \frac{\hbar^2k^2}{2m}+\Sigma(\mathbf{k},\frac{\hbar k^2}{2m})$, leads to

$$\frac{E(\tilde{\mathbf{k}})}{\hbar\omega_0} \approx \tilde{k}^2-\alpha\left[1+\frac{16T_0}{45\tilde{V}_0}\left(T_1+\frac{T_0}{6}\right)\right]\frac{\arcsin(\tilde{k})}{\tilde{k}}+\frac{2\alpha}{15\tilde{V}_0}\left(T_1-\frac{2T_0}{3}\right)^2\frac{\arcsin\left(\frac{\tilde{k}}{\sqrt{2}}\right)}{\tilde{k}}+\frac{4\alpha T_0^2}{45\tilde{V}_0}\frac{1}{\sqrt{1-\tilde{k}^2}}. \tag{75}$$

This energy dispersion can be expanded up to second order in $\tilde{k}$ to obtain the ground-state energy and effective mass of the polaron,

$$\frac{E_0}{\hbar\omega_0} = -\alpha-\frac{\sqrt{2}}{15}\frac{\alpha}{\tilde{V}_0}\left[T_1^2+\frac{4(2\sqrt{2}-1)}{3}T_0T_1+\frac{2(5\sqrt{2}+2)}{9}T_0^2\right]+O(\alpha^2), \tag{76}$$

$$\frac{m_{\text{eff}}}{m} = 1+\frac{\alpha}{6}+\frac{1}{90\sqrt{2}}\frac{\alpha}{\tilde{V}_0}\left[T_1^2+\frac{4(4\sqrt{2}-1)}{3}T_0T_1+\frac{4(11\sqrt{2}+1)}{9}T_0^2\right]+O(\alpha^2). \tag{77}$$

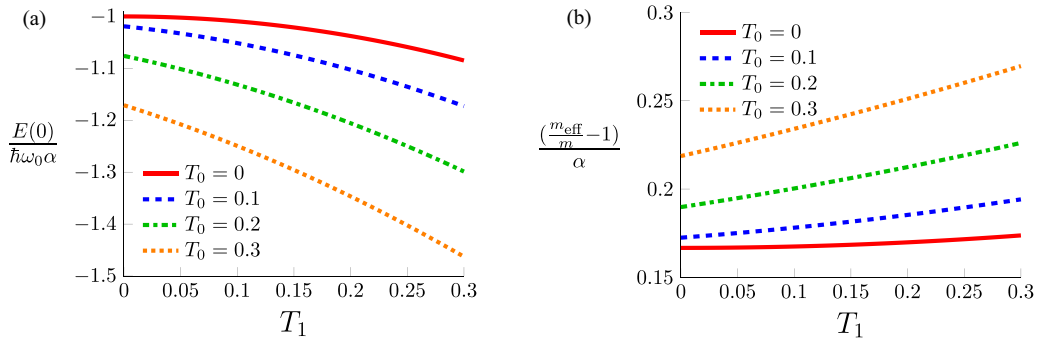

FIG. 3. (a) Ground-state energy and (b) effective mass of the polaron obtained through lowest-order perturbation theory, as a function of the anharmonic parameters T_0 and T_1. A typical value of $\tilde{V}_0 = 0.1$ was used: This corresponds to the dimensionless volume of the zinc-blende unit cell [31–33].

The first terms in these expressions are the well-known results for the ground-state energy and effective mass of the Fröhlich polaron. The remaining terms are the corrections due to the anharmonic terms (63) and (64). The correction terms are proportional to α and combinations of squares of the anharmonic parameters T_0 and T_1, in accordance with the results of [25]. We find a prefactor ${\tilde{V}_0}^{-1}$ from the renormalization of the integral (70), in contrast to the prefactor $\tilde{V}_0^{-\frac{2}{3}}$ found by Kussow [25]. This is because in [25] a different form for $V^{(1)}_{\mathbf{k},\mathbf{q}}$ is used, as will be discussed in Sec. V.

Figure 3 shows the ground-state energy and effective mass of the polaron in the small coupling limit $\alpha \lesssim 1$. It is clear that the three-phonon interaction $V^{(0)}_{\mathbf{k},\mathbf{q}}$ and the two-phonon emission/absorption amplitude $V^{(1)}_{\mathbf{k},\mathbf{q}}$ can both lower the ground-state energy and increase the effective mass quite significantly, even for relatively small values of T_0 and T_1.

IV. PATH-INTEGRAL TREATMENT

The results from the previous section are useful in the case of weak coupling ($\alpha \lesssim 1$). However, plenty of polar solids have stronger electron-phonon coupling. For this case, the ground-state energy of the polaron can be calculated using any of several variational methods, including the Lee-Low-Pines method [34], the Landau-Pekar method [2,35], and the Feynman path-integral method [26]. The Lee-Low-Pines and the Landau-Pekar methods both propose coherent phonon states as their variational ground state, which is inadequate for the description of the extended Hamiltonian (62)–(64). Therefore, we will calculate the ground-state energy using the path-integral method, which treats the phonons exactly and is known to give good results for the harmonic problem at all coupling strengths [36,37]. Since only path integrals that are quadratic in the phonon coordinates can be calculated exactly, we must limit ourselves to the case where $T_0 = 0$ and neglect the three-phonon terms; however, these can be treated separately and included in a renormalized phonon frequency [13–15].

A. Path integral over the phonons

The path-integral method has recently been applied to the Bose polaron in ultracold gases [8] where an interaction term similar to (64) is present; this derivation follows the same general idea. This part of the derivation is valid for general functions $\omega_{\mathbf{k}}$, $V^{(F)}_{\mathbf{k}}$, and $V^{(1)}_{\mathbf{k},\mathbf{q}}$. In the path-integral formalism, the partition sum Z at finite inverse temperature β can be written as a quantum statistical path integral over the electron and phonon coordinates,

$$Z = \int \mathcal{D}\mathbf{r}(\tau) \int \mathcal{D}q_{\mathbf{k}}(\tau) \times \exp\left\{-\frac{1}{\hbar}\int_0^{\hbar\beta} L[q_{\mathbf{k}}(\tau), \dot{q}_{\mathbf{k}}(\tau), \mathbf{r}(\tau), \dot{\mathbf{r}}(\tau)]d\tau\right\}, \tag{78}$$

where the imaginary-time Lagrangian L can be found by writing Eqs. (18) and (19) in terms of phonon coordinates $q_{\mathbf{k}}$ and $\dot{q}_{\mathbf{k}}$ instead of creation and annihilation operators, calculating the energy density again, and making the substitution $t \to -i\tau$. Introducing an arbitrary phonon mass m_{ph} and assuming $V^{(0)}_{\mathbf{k},\mathbf{q}} \approx 0$, the Lagrangian is given by

$$\begin{aligned} &L[q_{\mathbf{k}}(\tau), \dot{q}_{\mathbf{k}}(\tau), \mathbf{r}(\tau), \dot{\mathbf{r}}(\tau)] \\ &= \frac{m}{2}\dot{\mathbf{r}}^2 + \sum_{\mathbf{k}} \frac{m_{\text{ph}}}{2}\left(\dot{q}^*_{\mathbf{k}}\dot{q}_{\mathbf{k}} + \omega^2_{\mathbf{k}} q^*_{\mathbf{k}} q_{\mathbf{k}}\right) \\ &\quad + \text{Re}\left[\sum_{\mathbf{k}} \sqrt{\frac{2m_{\text{ph}}\omega_{\mathbf{k}}}{\hbar}} V^{(F)}_{\mathbf{k}} \rho_{\mathbf{k}} q_{\mathbf{k}}\right] \\ &\quad + \text{Re}\left[\sum_{\mathbf{k},\mathbf{k}'} \frac{2m_{\text{ph}}\sqrt{\omega_{\mathbf{k}}\omega_{\mathbf{k}'}}}{\hbar} V^{(1)}_{\mathbf{k},\mathbf{k}'} \rho_{\mathbf{k}-\mathbf{k}'} q_{\mathbf{k}} q^*_{\mathbf{k}'}\right]. \end{aligned} \tag{79}$$

This Lagrangian is quadratic in the phonon coordinates $q_{\mathbf{k}}(\tau)$, so its path integral can be evaluated exactly [8]. This is most easily done by expanding the phonon and electron coordinates in a Fourier-Matsubara series,

$$q_{\mathbf{k}}(\tau) = \sum_n c_{\mathbf{k},n} e^{i\omega_n \tau}, \tag{80}$$

$$\rho_{\mathbf{k}}(\tau) = \sum_n f_{\mathbf{k},n} e^{i\omega_n \tau}, \tag{81}$$

where the bosonic Matsubara frequencies are given by $\omega_n = \frac{2\pi n}{\hbar\beta}$. Then, the coefficients $c_{\mathbf{k},n}$ can be integrated over the complex plane to perform the path integral. If we consider

the pair $\{\mathbf{k}, n\}$ to be a single index, this integral will be a multivariate Gaussian integral, which has a well-known expression. A straightforward calculation yields that if we define the "matrix" A and the "vector" B as

$$A_{\mathbf{k},n,\mathbf{k}',n'} = \frac{m_{\text{ph}}}{2}(\omega_n^2 + \omega_{\mathbf{k}}^2)\delta_{\mathbf{k},\mathbf{k}'}\delta_{n,n'} + \frac{2m_{\text{ph}}\sqrt{\omega_{\mathbf{k}}\omega_{\mathbf{k}'}}}{\hbar}V^{(1)}_{\mathbf{k},\mathbf{k}'}f_{\mathbf{k}-\mathbf{k}',n-n'}, \tag{82}$$

$$B_{\mathbf{k},n} = \sqrt{\frac{2m_{\text{ph}}\omega_{\mathbf{k}}}{\hbar}}V^{(F)}_{\mathbf{k}}f_{\mathbf{k},n}, \tag{83}$$

then the path integral over the phonons can be written as follows:

$$\int \mathcal{D}q_{\mathbf{k}}(\tau)\exp\left\{-\frac{1}{\hbar}\int_0^{\hbar\beta} L[q_{\mathbf{k}}(\tau), \dot{q}_{\mathbf{k}}(\tau), \mathbf{r}(\tau), \dot{\mathbf{r}}(\tau)]d\tau\right\} \tag{84}$$

$$\sim \int_{\mathbb{C}} \exp\left[-\beta\,\text{Re}\left(\sum_{\mathbf{k},\mathbf{k}',n,n'} c_{\mathbf{k},n}A_{\mathbf{k},n,\mathbf{k}',n'}c^*_{\mathbf{k}',n'} + \sum_{\mathbf{k},n} B_{\mathbf{k},n}c_{\mathbf{k},n}\right)\right]dc_{\mathbf{k},n} \tag{85}$$

$$\sim \frac{1}{\sqrt{\det(A)}}\exp\left(\frac{m_{\text{ph}}\beta}{2\hbar^2}\sum_{\mathbf{k},n,\mathbf{k}',n'}\sqrt{\omega_{\mathbf{k}}\omega_{\mathbf{k}'}}V^{(F)*}_{\mathbf{k}}f^*_{\mathbf{k},n}A^{-1}_{\mathbf{k},n,\mathbf{k}',n'}f_{\mathbf{k}',n'}V^{(F)}_{\mathbf{k}'}\right). \tag{86}$$

The determinant in this expression can be rewritten in an exponential form, using $\det(A) = e^{\text{Tr}[\ln(A)]}$. To continue, the inverse and logarithm of the matrix A must be calculated, which cannot be done in closed form. However, since A is the sum of a diagonal matrix and an additional small term, we can use the series definitions for the inverse and the logarithm to continue. The prefactor can be obtained by comparing to the known case [38] where $\rho_{\mathbf{k}} = V^{(1)}_{\mathbf{k},\mathbf{k}'} = 0$. Additionally, expressions (80) and (81) can be used to convert our expressions back to imaginary time. All of these calculations are fairly straightforward and the final result can be written in terms of an effective action functional for only the electron,

$$Z = \left(\prod_{\mathbf{k}}\frac{1}{2\sinh(\frac{\hbar\beta\omega_{\mathbf{k}}}{2})}\right)\int \mathcal{D}\mathbf{r}(\tau)\exp\left\{-\frac{1}{\hbar}S_{\text{eff}}[\mathbf{r}(\tau)]\right\}, \tag{87}$$

$$S_{\text{eff}}[\mathbf{r}(\tau)] = \int_0^{\hbar\beta}\frac{1}{2}m\dot{\mathbf{r}}^2d\tau - \hbar\sum_{n=0}^{+\infty}(-1)^nO_n[\mathbf{r}(\tau)] - \hbar\sum_{n=1}^{+\infty}\frac{(-1)^n}{n}\tilde{O}_n[\mathbf{r}(\tau)]. \tag{88}$$

Similar to [8], the effective action is written is a series form, and the terms O_n and $\tilde{O}_n$ represent scattering processes. O_n and $\tilde{O}_n$ are both dimensionless functionals of $\mathbf{r}(\tau)$ of the nth order in $V^{(1)}_{\mathbf{k},\mathbf{q}}$, and are given explicitly by the following expressions:

$$O_n[\mathbf{r}(\tau)] := \frac{1}{8}\left(\frac{2}{\hbar}\right)^{n+2}\sum_{\mathbf{k}_1,\ldots,\mathbf{k}_{n+1}}\int_0^{\hbar\beta}d\tau_1\cdots\int_0^{\hbar\beta}d\tau_{n+2}V^{(F)*}_{\mathbf{k}_1}V^{(1)}_{\mathbf{k}_1,\mathbf{k}_2}\cdots V^{(1)}_{\mathbf{k}_n,\mathbf{k}_{n+1}}V^{(F)}_{\mathbf{k}_{n+1}}$$
$$\times\,\rho^*_{\mathbf{k}_1}(\tau_1)\rho_{\mathbf{k}_1-\mathbf{k}_2}(\tau_2)\cdots\rho_{\mathbf{k}_n-\mathbf{k}_{n+1}}(\tau_{n+1})\rho_{\mathbf{k}_{n+1}}(\tau_{n+2})G_{\mathbf{k}_1}(\tau_1-\tau_2)\cdots G_{\mathbf{k}_{n+1}}(\tau_{n+1}-\tau_{n+2}), \tag{89}$$

$$\tilde{O}_n[\mathbf{r}(\tau)] := \frac{1}{2}\left(\frac{2}{\hbar}\right)^{n}\sum_{\mathbf{k}_1,\ldots,\mathbf{k}_n}\int_0^{\hbar\beta}d\tau_1\cdots\int_0^{\hbar\beta}d\tau_nV^{(1)}_{\mathbf{k}_1,\mathbf{k}_2}V^{(1)}_{\mathbf{k}_2,\mathbf{k}_3}\cdots V^{(1)}_{\mathbf{k}_n,\mathbf{k}_1}$$
$$\times\,\rho_{\mathbf{k}_1-\mathbf{k}_2}(\tau_1)\rho_{\mathbf{k}_2-\mathbf{k}_3}(\tau_2)\cdots\rho_{\mathbf{k}_n-\mathbf{k}_1}(\tau_n)G_{\mathbf{k}_1}(\tau_n-\tau_1)G_{\mathbf{k}_2}(\tau_1-\tau_2)\cdots G_{\mathbf{k}_n}(\tau_{n-1}-\tau_n), \tag{90}$$

where we define the dimensionless phonon Green's function as

$$G_{\mathbf{k}}(\tau) := \frac{2\omega_{\mathbf{k}}}{\hbar\beta}\sum_n\frac{e^{i\omega_n\tau}}{\omega_n^2+\omega_{\mathbf{k}}^2} = \frac{\cosh\left[\omega_{\mathbf{k}}\left(\frac{\hbar\beta}{2}-|\tau|\right)\right]}{\sinh\left(\frac{\hbar\beta\omega_{\mathbf{k}}}{2}\right)} \quad (-\hbar\beta < \tau < \hbar\beta). \tag{91}$$

Some remarks must be made about the expressions (87) and (88) for the partition sum and the effective action. First, the prefactor in (87) is simply the partition sum of the free phonon field, which will contribute $\frac{\hbar\omega_{\mathbf{k}}}{2}$ to the ground-state energy for each phonon mode. This divergent ground-state energy does not contain the coordinate $\mathbf{r}(\tau)$ and can therefore be dropped. A similar statement can be made about $\tilde{O}_1[\mathbf{r}(\tau)]$. In [8], this term is dubbed the "vacuum polarization term" and is denoted by $\tilde{O}_0$ instead of $\tilde{O}_1$. From (90), one can see that it also does not depend on the electron coordinate,

$$\tilde{O}_1[\mathbf{r}(\tau)] = \beta\sum_{\mathbf{k}}V^{(1)}_{\mathbf{k},\mathbf{k}}\coth\left(\frac{\hbar\beta\omega_{\mathbf{k}}}{2}\right). \tag{92}$$

In our case, we have $V^{(1)}_{\mathbf{k},\mathbf{k}} = 0$, so the term is zero anyway: This means that in expression (88), we can let the second sum start at $n = 2$.

B. Variational principle for the free energy

So far, no approximations have been made other than $V^{(0)}_{\mathbf{k},\mathbf{q}} = 0$: The phonons have been treated exactly and the problem is reduced to the single path integral (87) over the electron coordinate. This path integral is too complicated to calculate analytically, even in the harmonic problem. However, the Jensen-Feynman variational inequality [26,38] can be used to estimate the free energy F of the problem. Given any model system with action $S_0[\mathbf{r}(\tau)]$, it holds that F is bounded by

$$F \leqslant F_0 + \frac{1}{\hbar\beta}\langle S - S_0\rangle, \tag{93}$$

where F_0 is the free energy of the model system, and the sharp brackets denote an expectation value with respect to this model system. It is common [8,26,39,40] to use a model system where the electron is coupled to a fictitious "phonon" mass M by a spring with spring constant MW^2: The mass M and the frequency W are variational parameters. This model system is quadratic in $\mathbf{r}(\tau)$, so it is possible to calculate the required expectation values. The action of this model system can be written in terms of only the electron coordinate by tracing out the fictitious phonon coordinate $\mathbf{Q}(\tau)$, yielding

$$\begin{aligned} S_0 = &\int_0^{\hbar\beta} \frac{m}{2}\dot{\mathbf{r}}(\tau)^2 d\tau + \frac{mW(\Omega^2 - W^2)}{8} \\ &\times \int_0^{\hbar\beta}\int_0^{\hbar\beta} \frac{\cosh\left[W\left(\frac{\hbar\beta}{2} - |\tau - \tau'|\right)\right]}{\sinh\left(\frac{W\hbar\beta}{2}\right)} \\ &\times |\mathbf{r}(\tau) - \mathbf{r}(\tau')|^2 d\tau d\tau', \end{aligned} \tag{94}$$

where $\Omega := W\sqrt{1 + \frac{M}{m}}$ replaces M as the variational parameter.

All the expectation values relevant to this article can be calculated from the memory function [8,39,40], which is given by

$$\langle \rho^*_{\mathbf{k}}(\tau)\rho_{\mathbf{k}}(\tau')\rangle := \exp\left[-\frac{\hbar}{2m}k^2 D(\tau - \tau')\right], \tag{95}$$

where the function $D(\tau)$ is defined as

$$D(\tau) := \frac{W^2}{\Omega^2}\left(|\tau| - \frac{|\tau|^2}{\hbar\beta}\right) + \frac{1}{\Omega}\left(1 - \frac{W^2}{\Omega^2}\right)\frac{\cosh\left(\Omega\frac{\hbar\beta}{2}\right) - \cosh\left[\Omega\left(\frac{\hbar\beta}{2} - |\tau|\right)\right]}{\sinh\left(\Omega\frac{\hbar\beta}{2}\right)}. \tag{96}$$

From this expectation value, the free energy F_0 and the expectation value $\langle S_0\rangle$ can be evaluated exactly. These quantities only depend on the model system and not on the effective action (88), and have been calculated before [8,39–41]. Using these in the Jensen-Feynman inequality (93), the variational upper bound for the polaron free energy can be written as

$$F \leqslant \frac{3}{\beta}\ln\left(\frac{W}{\Omega}\frac{\sinh\left(\frac{\hbar\beta\Omega}{2}\right)}{\sinh\left(\frac{\hbar\beta W}{2}\right)}\right) - \frac{3}{4}\hbar\Omega\left(1 - \frac{W^2}{\Omega^2}\right)\left[\coth\left(\frac{\hbar\beta\Omega}{2}\right) - \frac{2}{\hbar\beta\Omega}\right] - \frac{1}{\beta}\sum_{n=0}^{+\infty}(-1)^n\langle O_n\rangle - \frac{1}{\beta}\sum_{n=2}^{+\infty}\frac{(-1)^n}{n}\langle\tilde{O}_n\rangle. \tag{97}$$

Finally, taking the zero-temperature limit ($\beta \to +\infty$), the following variational principle for the ground-state energy of the polaron is obtained:

$$\frac{E(0)}{\hbar\omega_0} \leqslant \frac{3}{4\omega_0}\frac{(\Omega - W)^2}{\Omega} - \lim_{\beta\to+\infty}\frac{1}{\hbar\omega_0\beta}\sum_{n=0}^{+\infty}(-1)^n\langle O_n\rangle - \lim_{\beta\to+\infty}\frac{1}{\hbar\omega_0\beta}\sum_{n=2}^{+\infty}\frac{(-1)^n}{n}\langle\tilde{O}_n\rangle. \tag{98}$$

The problem is reduced to calculating the expectation values $\langle O_n\rangle$ and $\langle\tilde{O}_n\rangle$ with respect to the model action using Eq. (95). These expectation values will be functions of the variational parameters W and Ω. Once these expectation values are calculated, (98) can be minimized with respect to W and Ω to obtain an estimate of the polaron ground-state energy.

C. Calculation of the expectation values

The calculation of the general expectation values $\langle O_n\rangle$ and $\langle\tilde{O}_n\rangle$ is a hard problem for the interaction strengths given by (54) and (56), mostly due to the high-dimensional integrals that appear. In [8], a random phase approximation is made that allows analytical resummation of expression (98) if the interaction strength factorizes as $V^{(1)}_{\mathbf{k},\mathbf{q}} \sim V^{(F)}_{\mathbf{k}}V^{(F)}_{\mathbf{q}}$. Since this is not the case for (56), we will instead consider the case where T_1 is small and calculate only the contributions to the ground-state energy up to the order of T_1^2.

First, we note that for the interaction strengths given by (54)–(56), the odd order expectation values $\langle O_{2n+1}\rangle$ and $\langle\tilde{O}_{2n+1}\rangle$ are zero due to antisymmetry. This means only $\langle O_0\rangle$, $\langle O_2\rangle$, and $\langle\tilde{O}_2\rangle$ have to be calculated. $\langle O_0\rangle$ is the contribution from the Fröhlich action and can be calculated straightforwardly using (95). Similarly, $\langle\tilde{O}_2\rangle$ can be calculated using (95) and the result from the Appendix. The results are

$$\langle O_0\rangle = \hbar\omega_0\beta\frac{\alpha}{\sqrt{\pi}}\int_0^{\frac{\hbar\beta}{2}}\frac{G(\tau)}{\sqrt{\frac{D(\tau)}{\omega_0}}}d\tau, \tag{99}$$

$$\langle\tilde{O}_2\rangle = \hbar\omega_0\beta\frac{4}{15\sqrt{\pi}}\frac{\alpha T_1^2}{\tilde{V}_0}\int_0^{\frac{\hbar\beta}{2}}\frac{G(\tau)^2}{\sqrt{\frac{D(\tau)}{\omega_0}}}d\tau. \tag{100}$$

As before, the volume of the unit cell, $\tilde{V}_0$, appears to renormalize the divergent integral (70), so $\langle\tilde{O}_2\rangle$ will be large in the continuum limit. $\langle O_2\rangle$ is also of the order of T_1^2 and is quite difficult to compute, but does not contain this factor $\tilde{V}_0$ and can therefore be neglected. With these expectation values, Eq. (98)

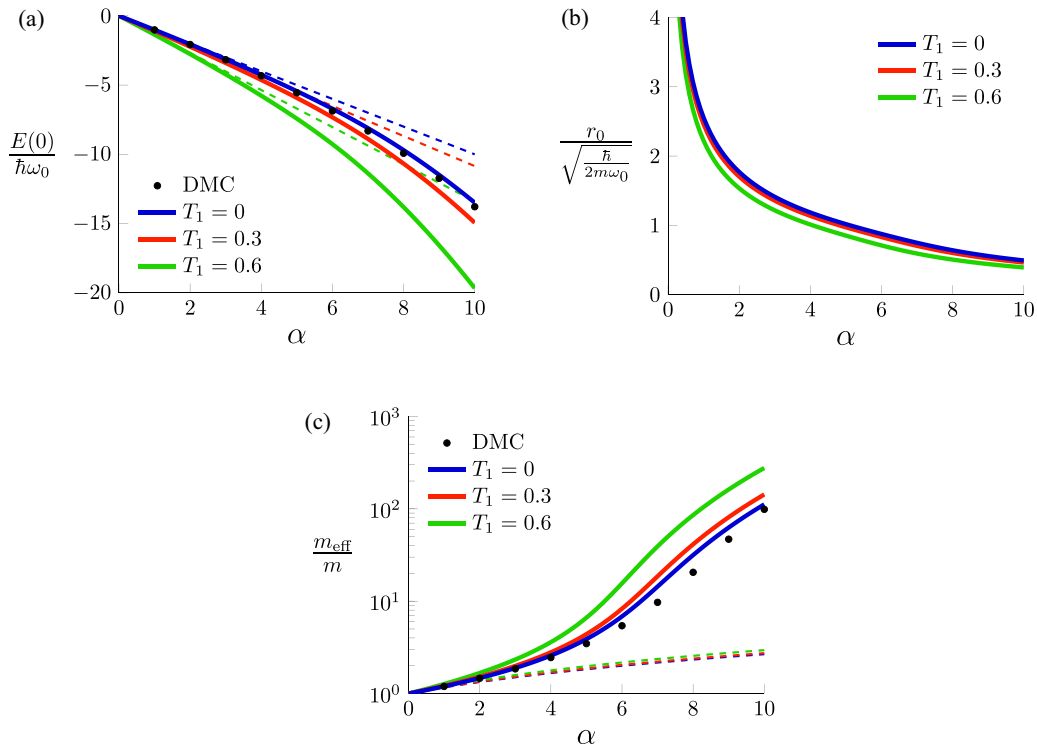

FIG. 4. (a) Ground-state energy, (b) radius, and (c) effective mass of the polaron from Feynman's variational method with $T_0 = 0$ and $\tilde{V}_0 = 0.1$. Dashed lines represent the perturbation theory result (76) and (77). Note that the effective mass is plotted on a logarithmic scale. (a) and (c) also show the result obtained by the diagrammatic Monte Carlo method [37] for the harmonic problem ($T_1 = 0$). This shows the remarkable accuracy of the Feynman variational method for the ground-state energy at all coupling strengths, but also reveals the inaccuracy of the effective mass in the intermediate coupling regime.

for the variational upper bound becomes

$$\frac{E_0}{\hbar\omega_0} \lesssim \frac{3}{4}\frac{(v-w)^2}{v} - \frac{\alpha}{\sqrt{\pi}}\int_0^{+\infty} \frac{e^{-\sigma} + \frac{2}{15}\frac{T_1^2}{\tilde{V}_0}e^{-2\sigma}}{\sqrt{\frac{w^2}{v^2}\sigma + \left(1-\frac{w^2}{v^2}\right)\frac{1-e^{-v\sigma}}{v}}}d\sigma, \quad (101)$$

where $w := \frac{W}{\omega_0}$ and $v := \frac{\Omega}{\omega_0}$ are the new dimensionless variational parameters. The result immediately reduces to the Feynman ground-state energy [26] if $T_1 = 0$. It must be noted that the variational inequality may no longer hold since several terms which may be positive were neglected in (98).

The ground-state energy is obtained by numerically minimizing Eq. (101): The result is shown in Fig. 4(a). In the weak coupling limit $\alpha \ll 1$, the ground-state energy is minimized by $v = w$ [26]: Then (101) reduces to the perturbation theory result (76) with $T_0 = 0$, as can be seen in Fig. 4(a). Similar to the perturbation theory result, the ground-state energy is significantly lowered by the anharmonic interaction. This effect is even more dramatic in the strong coupling regime $\alpha \gg 1$.

Once the variational parameters v and w are chosen in such a way that they minimize the ground-state energy, they may be used to calculated a range of other properties of the polaron. One of these is the polaron radius, which may be defined in several different ways. Here, we define it using the average displacement of the relative coordinate in the model system [39,40,42],

$$r_0 = \sqrt{\langle|\mathbf{r}(\tau) - \mathbf{Q}(\tau)|^2\rangle} = \sqrt{\frac{\hbar}{2m\omega_0}}\frac{3v}{v^2-w^2}\coth\left(\frac{\hbar\beta\omega_0}{2}v\right). \quad (102)$$

Another is the effective mass, which can be estimated by replacing the memory function (95) by the following expression, where $\mathbf{u}$ represents the velocity of the electron [8,26,39,40]:

$$\langle\rho_{\mathbf{k}}^*(\tau)\rho_{\mathbf{k}}(\tau')\rangle := \exp\left[-\frac{\hbar}{2m}k^2 D(\tau-\tau') + i\mathbf{k}\cdot\mathbf{u}\,(\tau-\tau')\right]. \quad (103)$$

The calculations have to be redone with this form of the memory function, up to the order of u^2. Eventually, the ground-state energy will gain an extra term of the form $\frac{1}{2}m_{\text{eff}}u^2$, where the prefactor can be interpreted as the effective mass of the polaron. The resulting expression is

$$\frac{m_{\text{eff}}}{m} = 1 + \frac{\alpha}{3\sqrt{\pi}}\int_0^{+\infty} \frac{\sigma^2\left(e^{-\sigma} + \frac{2}{15}\frac{T_1^2}{\tilde{V}_0}e^{-2\sigma}\right)}{\left[\frac{w^2}{v^2}\sigma + \left(1-\frac{w^2}{v^2}\right)\frac{1-e^{-v\sigma}}{v}\right]^{\frac{3}{2}}}d\sigma. \quad (104)$$

The polaron radius and the effective mass are shown in Figs. 4(b) and 4(c). Just like the ground-state energy, the effective mass is significantly increased by T_1 in the strong

coupling regime. As is known from Fröhlich polaron theory, the effective mass increases strongly in the intermediate coupling regime. When the anharmonic introduction is introduced, this strong increase in the effective mass shifts to slightly lower values of α.

The introduction of the anharmonic electron-phonon coupling decreases the polaron radius, as can be intuitively expected. The polaron radius diverges in the weak coupling limit since the polaron becomes free, and is therefore completely delocalized. This is different from some other definitions of the polaron radius, where it is interpreted as the spatial extent of the induced charge density [34,43] and therefore remains constant as $\alpha \to 0$.

V. DISCUSSION AND CONCLUSIONS

The main result of this paper is the Hamiltonian (60)–(64) for a single polaron in a cubic crystal with third-order anharmonicity. The derivation is presented in such a way that it can be straightforwardly generalized to the case of multiple polarons, general crystal symmetries, and higher-order anharmonic terms. If cubic symmetry is assumed, the harmonic interaction strengths and the phonon frequency are isotropic and reduce to the Fröhlich form, as expected [10]. However, it is not enough to make the anharmonic interaction strengths (55)–(58) isotropic, and tensor notation or index notation is still required despite the cubic symmetry.

Hamiltonians of the form (60)–(64), including the anharmonic interactions, can be found in other areas of physics. A notable example is the Bose polaron Hamiltonian, describing impurities in ultracold Bose gases under the Bogoliubov approximation [7,8]. The Hamiltonians only differ in their different expressions of the interaction strengths $V_{\mathbf{k}}^{(F)}$, $V_{\mathbf{k},\mathbf{q}}^{(0)}$, and $V_{\mathbf{k},\mathbf{q}}^{(1)}$.

To obtain the Hamiltonian (60)–(64), we have made several drastic assumptions: the material must belong to either of the point groups 23 or $\bar{4}3m$, and the primitive unit cell must contain only two atoms. Regardless, III-V semiconductors such as BN, BP, AlN, and AlP all exist in the zinc-blende structure and therefore satisfy all of the above assumptions. In addition, these semiconductors display significant anharmonicity [27–29] since their ions are relatively light. In any of these materials, anharmonic polarons corresponding to the Hamiltonian (60)–(64) may be experimentally observed, for example by measuring the midinfrared optical conductivity. The Fröhlich electron-phonon coupling (62) gives rise to an absorption peak around $\omega \approx \omega_0$ [44–46]. Since the anharmonic electron-phonon coupling (64) involves the simultaneous creation of two phonons [see Fig. 2(b)], it will give rise to a secondary peak around $\omega \approx 2\omega_0$. This secondary peak serves as a fingerprint for anharmonicity of the form given by (63) and (64).

The Hamiltonian (60)–(64) for a single polaron contains two unknown dimensionless material parameters T_0 and T_1, which characterize the relative strength of the two anharmonic interactions. Although T_0 can, in theory, be linked to the Grüneisen constant γ_{LO} of the longitudinal optical phonons, we found no way to directly link T_0 and T_1 to experimentally available material parameters. Therefore, even an order of magnitude estimate of T_0 and T_1, and any quantitative comparison to experiments, is difficult. In addition to this, all treatments of anharmonic polarons besides that of Kussow [25] have focused on small polarons [22–24], so any comparison with these results would have to be qualitative anyway.

We based our work on Kussow [25], who also derives a Hamiltonian of the form (64). Our expression for the interaction strength (56) does not match the expression in [25], for two reasons. First, [25] uses the following form for the tensor $A_{ijk}^{(1)}$:

$$A_{ijl}^{(1)} = A_1 \delta_{ijl}, \qquad \text{where } \delta_{ijl} = \begin{cases} 1 & \text{if } i=j=l \\ 0 & \text{otherwise,} \end{cases} \tag{105}$$

instead of the correct form (37). Additionally, the final integral in their derivation (Eq. (40) in [25]) is incorrectly calculated using Green's theorem. Despite this, the Hamiltonian in [25] is still of the correct order of magnitude, so their results should still be qualitatively correct. Indeed, in [25] it is also concluded that the ground-state energy is lowered and the effective mass is increased by the anharmonic interaction, and that the transition to a small polaron occurs at lower values of α if the anharmonic interaction is present. These qualitative results are also seen for the small polaron if an asymmetric on-site potential is used [22]. Interestingly, the effects of anharmonicity seem to be reversed if a quartic potential is used [23] instead of a cubic potential. It could be interesting to see if similar results are found if the internal energy (6) is expanded up to fourth order and a crystal with inversion symmetry is considered.

The derived Hamiltonian (22) is well suited for the calculation of further anharmonic large polaron properties since the interaction strengths are analytical and depend on only one dimensionless parameter each. In addition, it is a direct generalization of the Fröhlich Hamiltonian, meaning most theoretical techniques for solving the Fröhlich Hamiltonian can be used for this Hamiltonian as well (except, perhaps, the Lee-Low-Pines and Landau-Pekar methods, as discussed in Sec. IV). For example, the electron mobility/AC conductivity/optical response can be calculated semianalytically using several different methods [45,47,48]. The optical response is of great significance for high-pressure hydride and metallic hydrogen experiments [16,17,20,21,49] and can even be used to determine the superconducting transition [50]. Using this Hamiltonian, it is also possible to investigate bipolaron formation [51], which has been proposed as a possible pairing mechanism for superconductivity. While bipolarons can only occur at $\alpha > 6.8$ in the harmonic approximation [51], the increased electron-phonon interaction energy suggests a wider stability regime in the anharmonic case. Further calculations may indicate whether bipolarons can occur for values of α, T_0, and T_1 corresponding to a realistic material.

ACKNOWLEDGMENTS

This research was funded by the University Research Fund (BOF) of the Antwerp University (project ID: 38499). We would like to thank T. Ichmoukhamedov, T. Hahn, and S. Ragni for many interesting discussions. We also thank C. Franchini and G. Kresse for their longstanding collaboration

with our research group, and for agreeing to calculate the anharmonic coefficients from first principles.

APPENDIX: INTEGRAL OVER THE ANHARMONIC INTERACTION STRENGTH

During the calculation of the polaron energy using both perturbation theory and the path-integral formalism, we encountered the following sum:

$$\mathcal{I} = \sum_{\mathbf{k}} \left| \frac{6V^{(0)}_{\mathbf{q},\mathbf{k}}}{\hbar\omega_0} \right|^2. \tag{A1}$$

Unlike the other integrals in this article, the calculation of the above integral is not quite straightforward and deserves some further explanation.

The sum can be transformed into an integral using $\sum_{\mathbf{k}} \to \frac{V}{(2\pi)^3}\int d^3\mathbf{k}$. Then, we can plug in expression (55) for $V^{(0)}_{\mathbf{q},\mathbf{k}}$ to obtain

$$\mathcal{I} = \frac{T_0^2 a_p^3}{(2\pi)^3} \int \left(\mathcal{E}_{ijl} n_i^{\mathbf{k}} n_j^{\mathbf{k}-\mathbf{q}} n_l^{\mathbf{q}}\right)^2 d^3\mathbf{k}, \tag{A2}$$

where the indices i, j, l are summed over the values $\{x, y, z\}$. First, we note that the integration domain is very large and the vector $\mathbf{q}$ is finite. This allows us to replace $n_j^{\mathbf{k}-\mathbf{q}}$ by $n_j^{\mathbf{k}}$,

$$\mathcal{I} = \frac{T_0^2 a_p^3}{(2\pi)^3} \int \left(\mathcal{E}_{ijl} n_i^{\mathbf{k}} n_j^{\mathbf{k}} n_l^{\mathbf{q}}\right)^2 d^3\mathbf{k}. \tag{A3}$$

Formally, this can be justified by substituting $\mathbf{k} \to a\mathbf{K}$ for some large value a: This substitution makes $\mathbf{q}$ negligibly small compared to $a\mathbf{K}$, but otherwise leaves the integral invariant since $n_i^{a\mathbf{K}} = n_i^{\mathbf{K}}$. More intuitively, the following argument can be used: Since the integrand remains finite as $|\mathbf{k}| \to +\infty$, the integral will be dominated by the domain in which $|\mathbf{k}| \gg |\mathbf{q}|$, and in this domain the vector $\mathbf{k} - \mathbf{q}$ and the vector $\mathbf{k}$ approximately have the same direction.

The volume element $d^3\mathbf{k}$ can now be written in spherical coordinates, and the radial and angular integrals can be split:

$$\mathcal{I} = \frac{T_0^2 a_p^3}{(2\pi)^3} \mathcal{E}_{ijl}\mathcal{E}_{abc} n_l^{\mathbf{q}} n_c^{\mathbf{q}} \int n_i^{\mathbf{k}} n_j^{\mathbf{k}} n_a^{\mathbf{k}} n_b^{\mathbf{k}} d^3\mathbf{k} \tag{A4}$$

$$= \frac{T_0^2 a_p^3}{(2\pi)^3} \mathcal{E}_{ijl}\mathcal{E}_{abc} n_l^{\mathbf{q}} n_c^{\mathbf{q}} \left(\int k^2 dk\right) \times \left[\int_0^{\pi}\int_0^{2\pi} n_i n_j n_a n_b \sin(\theta) d\theta d\varphi\right], \tag{A5}$$

where $\mathbf{n} = \mathbf{n}(\theta, \varphi)$ is a unit vector in the direction defined by the angles θ and φ. Its components are given by

$$n_x(\theta, \varphi) := \sin(\theta)\cos(\varphi), \tag{A6}$$

$$n_y(\theta, \varphi) := \sin(\theta)\sin(\varphi), \tag{A7}$$

$$n_z(\theta, \varphi) := \cos(\theta). \tag{A8}$$

The angular integral is a special case of the following integral identity [52]:

$$\int_0^{\pi}\int_0^{2\pi} n_{i_1} n_{i_2} \ldots n_{i_\ell} \sin(\theta) d\theta d\varphi = \begin{cases} \frac{4\pi}{\ell+1}\delta_{(i_1 i_2}\delta_{i_3 i_4}\ldots\delta_{i_{\ell-1} i_\ell)} & (\ell \text{ even}) \\ 0 & (\ell \text{ odd}). \end{cases} \tag{A9}$$

Then expression (A5) becomes

$$\mathcal{I} = \frac{T_0^2 a_p^3}{5(2\pi)^3} \delta_{(ij}\delta_{ab)} \mathcal{E}_{ijl}\mathcal{E}_{abc} n_l^{\mathbf{q}} n_c^{\mathbf{q}} \left(4\pi \int k^2 dk\right). \tag{A10}$$

The contractions over the indices i, j, a, and b can now be performed, using the fact that $\delta_{(ij}\delta_{ab)}\mathcal{E}_{ijl}\mathcal{E}_{abc} = \frac{4}{3}\delta_{lc}$. Then the integral becomes

$$\mathcal{I} = \frac{4T_0^2 a_p^3}{15(2\pi)^3} \mathbf{n}^{\mathbf{q}} \cdot \mathbf{n}^{\mathbf{q}} \int k^2 dk, \tag{A11}$$

$$\mathcal{I} = \frac{4T_0^2}{15} \times \frac{a_p^3}{(2\pi)^3}\left[4\pi \int k^2 dk\right]. \tag{A12}$$

If we assume $k \in [0, +\infty]$, the radial integral obviously diverges. However, physically, we only expect wave vectors in the first Brillouin zone to be relevant. Since we work in the continuum limit, the first Brillouin zone will be large, but not infinite, and we can use the volume of the first Brillouin zone as a Debye cutoff for the radial integral over k. The quantity between square brackets should equal the volume of the first Brillouin zone, which is equal to $\frac{(2\pi)^3}{V_0}$, where V_0 is the volume of the unit cell. Therefore, we finally find

$$\mathcal{I} = \sum_{\mathbf{k}} \left| \frac{6V^{(0)}_{\mathbf{q},\mathbf{k}}}{\hbar\omega_0} \right|^2 = \frac{4T_0^2}{15\tilde{V}_0}, \tag{A13}$$

where we defined $\tilde{V}_0 := V_0/a_p^3$ as in Eq. (71). This is the result we presented in the main text.

[1] L. D. Landau, Electron motion in crystal lattices, Phys. Z. Sowjet. **3**, 664 (1933).

[2] L. D. Landau and S. I. Pekar, Effective mass of a polaron, Zh. Eksp. Teor. Fiz. **18**, 419 (1948).

[3] E. L. Nagaev, Spin polaron theory for magnetic semiconductors with narrow bands, Phys. Status Solidi B **65**, 11 (1974).

[4] J. Koepsell, J. Vijayan, P. Sompet, F. Grusdt, T. A. Hilker, E. Demler, G. Salomon, I. Bloch, and C. Gross, Imaging magnetic polarons in the doped FermiHubbard model, Nature (London) **572**, 358 (2019).

[5] O. Verzelen, R. Ferreira, and G. Bastard, Excitonic Polarons in Semiconductor Quantum Dots, Phys. Rev. Lett. **88**, 146803 (2002).

[6] N. B. Jørgensen, L. Wacker, K. T. Skalmstang, M. M. Parish, J. Levinsen, R. S. Christensen, G. M. Bruun, and J. J. Arlt, Observation of Attractive and Repulsive Polarons in a Bose-Einstein Condensate, Phys. Rev. Lett. **117**, 055302 (2016).

[7] Y. E. Shchadilova, R. Schmidt, F. Grusdt, and E. Demler, Quantum Dynamics of Ultracold Bose Polarons, Phys. Rev. Lett. **117**, 113002 (2016).

[8] T. Ichmoukhamedov and J. Tempere, Feynman path-integral treatment of the Bose polaron beyond the Fröhlich model, Phys. Rev. A **100**, 043605 (2019).
[9] A. Schirotzek, C.-H. Wu, A. Sommer, and M. W. Zwierlein, Observation of Fermi Polarons in a Tunable Fermi Liquid of Ultracold Atoms, Phys. Rev. Lett. **102**, 230402 (2009).
[10] H. Fröhlich, Electrons in lattice fields, Adv. Phys. **3**, 325 (1954).
[11] F. Grusdt, Y. E. Shchadilova, A. N. Rubtsov, and E. Demler, Renormalization group approach to the Fröhlich polaron model: application to impurity-BEC problem, Sci. Rep. **5**, 12124 (2015).
[12] F. Grusdt, R. Schmidt, Y. E. Shchadilova, and E. Demler, Strong-coupling Bose polarons in a Bose-Einstein condensate, Phys. Rev. A **96**, 013607 (2017).
[13] I. Errea, M. Calandra, and F. Mauri, First-Principles Theory of Anharmonicity and the Inverse Isotope Effect in Superconducting Palladium-Hydride Compounds, Phys. Rev. Lett. **111**, 177002 (2013).
[14] I. Errea, M. Calandra, and F. Mauri, Anharmonic free energies and phonon dispersions from the stochastic self-consistent harmonic approximation: Application to platinum and palladium hydrides, Phys. Rev. B **89**, 064302 (2014).
[15] I. Errea, M. Calandra, C. J. Pickard, J. Nelson, R. J. Needs, Y. Li, H. Liu, Y. Zhang, Y. Ma, and F. Mauri, High-Pressure Hydrogen Sulfide from First Principles: A Strongly Anharmonic Phonon-Mediated Superconductor, Phys. Rev. Lett. **114**, 157004 (2015).
[16] A. Drozdov, M. Eremets, I. Troyan, V. Ksenofontov, and S. I. Shylin, Conventional superconductivity at 203 kelvin at high pressures in the sulfur hydride system, Nature (London) **525**, 73 (2015).
[17] M. Somayazulu, M. Ahart, A. K. Mishra, Z. M. Geballe, M. Baldini, Y. Meng, V. V. Struzhkin, and R. J. Hemley, Evidence for Superconductivity above 260 K in Lanthanum Superhydride at Megabar Pressures, Phys. Rev. Lett. **122**, 027001 (2019).
[18] E. Snider, N. Dasenbrock-Gammon, R. McBride, M. Debessai, H. Vindana, K. Vencatasamy, K. V. Lawler, A. Salamat, and R. P. Dias, Room-temperature superconductivity in a carbonaceous sulfur hydride, Nature (London) **586**, 373 (2020).
[19] N. W. Ashcroft, Metallic Hydrogen: A High-Temperature Superconductor, Phys. Rev. Lett. **21**, 1748 (1968).
[20] R. P. Dias and I. F. Silvera, Observation of the Wigner-Huntington transition to metallic hydrogen, Science **355**, 715 (2017).
[21] P. Loubeyre, F. Occelli, and P. Dumas, Observation of a first order phase transition to metal hydrogen near 425 gpa, arXiv:1906.05634.
[22] Y. Zolotaryuk, P. L. Christiansen, and J. J. Rasmussen, Polaron dynamics in a two-dimensional anharmonic Holstein model, Phys. Rev. B **58**, 14305 (1998).
[23] N. K. Voulgarakis and G. P. Tsironis, Stationary and dynamical properties of polarons in the anharmonic Holstein model, Phys. Rev. B **63**, 014302 (2000).
[24] M. G. Velarde, From polaron to solectron: The addition of nonlinear elasticity to quantum mechanics and its possible effect upon electric transport, J. Comput. Appl. Math. **233**, 1432 (2010).
[25] A.-G. Kussow, Large polaron in an anharmonic crystal lattice, Int. J. Mod. Phys. B **23**, 19 (2009).
[26] R. P. Feynman, Slow electrons in a polar crystal, Phys. Rev. **97**, 660 (1955).
[27] B. G. A. Brito, L. C. DaSilva, G.-Q. Hai, and L. Cândido, Anharmonic quantum effects in cubic boron nitride crystal by path integral monte carlo simulations, Phys. Status Solidi B **256**, 1900164 (2019).
[28] N. Shulumba, Z. Raza, O. Hellman, E. Janzén, I. A. Abrikosov, and M. Odén, Impact of anharmonic effects on the phase stability, thermal transport, and electronic properties of AlN, Phys. Rev. B **94**, 104305 (2016).
[29] K. Yaddanapudi, First-principles study of structural phase transformation and dynamical stability of cubic AlN semiconductors, AIP Adv. **8**, 125006 (2018).
[30] V. L. Gurevich, Transport in phonon systems, *Transport in Phonon Systems* (Elsevier Science, Amsterdam, 1986).
[31] A. Fairbrother, V. Izquierdo-Roca, X. Fontané, M. Ibáñez, A. Cabot, E. Saucedo, and A. Pérez-Rodríguez, ZnS grain size effects on near-resonant Raman scattering: optical nondestructive grain size estimation, CrystEngComm **16**, 4120 (2014).
[32] F. Opoku, K. K. Govender, C. G. C. E. van Sittert, and P. P. Govender, Understanding the mechanism of enhanced charge separation and visible light photocatalytic activity of modified wurtzite ZnO with nanoclusters of ZnS and graphene oxide: from a hybrid density functional study, New J. Chem. **41**, 8140 (2017).
[33] J. R. Rumble, T. J. Bruno, and M. Doa, *CRC Handbook of Chemistry and Physics*, 101st ed. (CRC Press, Boca Raton, FL, 2020).
[34] T. D. Lee, F. E. Low, and D. Pines, The motion of slow electrons in a polar crystal, Phys. Rev. **90**, 297 (1953).
[35] W. Casteels, T. Van Cauteren, J. Tempere, and J. T. Devreese, Strong coupling treatment of the polaronic system consisting of an impurity in a condensate, Laser Phys. **21**, 1480 (2011).
[36] N. V. Prokof'ev and B. V. Svistunov, Polaron Problem by Diagrammatic Quantum Monte Carlo, Phys. Rev. Lett. **81**, 2514 (1998).
[37] T. Hahn, S. Klimin, J. Tempere, J. T. Devreese, and C. Franchini, Diagrammatic Monte Carlo study of Fröhlich polaron dispersion in two and three dimensions, Phys. Rev. B **97**, 134305 (2018).
[38] H. Kleinert, Path integrals in quantum mechanics, statistics, polymer physics, and financial markets, *Path Integrals in Quantum Mechanics, Statistics, Polymer Physics, and Financial Markets*, 5th ed. (EBL-Schweitzer, World Scientific, Singapore, 2009).
[39] J. Tempere, W. Casteels, M. K. Oberthaler, S. Knoop, E. Timmermans, and J. T. Devreese, Feynman path-integral treatment of the BEC-impurity polaron, Phys. Rev. B **80**, 184504 (2009), Erratum: [40].
[40] W. Casteels, J. Tempere, M. K. Oberthaler, S. Knoop, E. Timmermans, and J. T. Devreese, Erratum: Feynman path-integral treatment of the BEC-impurity polaron, Phys. Rev. B **87**, 099903(E) (2013).
[41] R. P. Feynman, Statistical mechanics: A set of lectures, *Statistical Mechanics: A Set Of Lectures* (Addison-Wesley, Reading, MA, 1990).
[42] T. D. Schultz, Slow electrons in polar crystals: self-energy, mass, and mobility, Phys. Rev. **116**, 526 (1959).

[43] V. Fedyanin and C. Rodriguez, Path integral approach to polaron mass and radius at finite temperatures, Physica A **112**, 615 (1982).

[44] H. Finkenrath, N. Uhle, and W. Waidelich, The influence of phonons and polarons on the infrared absorption of cadmium oxide, Solid State Commun. **7**, 11 (1969).

[45] J. Tempere and J. T. Devreese, Optical absorption of an interacting many-polaron gas, Phys. Rev. B **64**, 104504 (2001).

[46] J. L. M. van Mechelen, D. van der Marel, C. Grimaldi, A. B. Kuzmenko, N. P. Armitage, N. Reyren, H. Hagemann, and I. I. Mazin, Electron-Phonon Interaction and Charge Carrier Mass Enhancement in $SrTiO_3$, Phys. Rev. Lett. **100**, 226403 (2008).

[47] R. P. Feynman, R. W. Hellwarth, C. K. Iddings, and P. M. Platzman, Mobility of slow electrons in a polar crystal, Phys. Rev. **127**, 1004 (1962).

[48] F. M. Peeters and J. T. Devreese, Impedance function of large polarons: An alternative derivation of the Feynman-Hellwarth-Iddings-Platzman theory, Phys. Rev. B **28**, 6051 (1983).

[49] M. Zaghoo, A. Salamat, and I. F. Silvera, Evidence of a first-order phase transition to metallic hydrogen, Phys. Rev. B **93**, 155128 (2016).

[50] J. P. Carbotte, E. J. Nicol, and T. Timusk, Detecting Superconductivity in the High Pressure Hydrides and Metallic Hydrogen from Optical Properties, Phys. Rev. Lett. **121**, 047002 (2018).

[51] G. Verbist, F. M. Peeters, and J. T. Devreese, Large bipolarons in two and three dimensions, Phys. Rev. B **43**, 2712 (1991).

[52] K. S. Thorne, Multipole expansions of gravitational radiation, Rev. Mod. Phys. **52**, 299 (1980).